Journal of Energy Storage 61 (2023) 106643

Contents lists available at ScienceDirect

Journal of Energy Storage

journal homepage: www.elsevier.com/locate/est

Research Papers

Suitability assessment of high-power energy storage technologies for offshore oil and gas platforms: A life cycle cost perspective

Ayotunde A. Adeyemo [a,*], Erick Alves [a], Francesco Marra [c], Danilo Brandao [d], Elisabetta Tedeschi [a,b]

[a] Department of Electric Energy, Norwegian University of Science and Technology (NTNU), O.S. Bragstads Plass 2E, 7034 Trondheim, Norway
[b] Department of Industrial Engineering, University of Trento, Italy
[c] Equinor Research Centre, Arkitekt Ebbells veg 10, 7053 Ranheim, Norway
[d] Graduate Program in Electrical Engineering, Universidade Federal de Minas Gerais (UFMG), Belo Horizonte 31270-901, Brazil

ARTICLE INFO

Keywords:
Offshore oil and gas platform
Technology suitability assessment
Energy storage
Supercapacitors
Lithium-ion batteries
Flywheels
Superconducting magnetic energy storage

ABSTRACT

This paper presents a technology suitability assessment (TSA) of high-power energy storage (ES) systems for application in isolated power systems, which is demonstrated through the case of offshore oil and gas platforms (OOGPs). OOGPs operate in very harsh environmental conditions (with limited weight and space), and this requires a specific assessment of which ES technologies are suitable for this application. This work presents a TSA procedure to address this problem. ES can be sized to provide many services. In this paper the focus is on primary frequency control, but the proposed approach can be extended to other services. The ES technologies assessed in detail include flywheels, supercapacitors (SCs), superconducting magnetic energy storage (SMES) and lithium-ion (Li-ion) batteries, which are critically selected from a broader pool of alternatives. A life cycle cost perspective is presented using the case study of an OOGP in the North Sea. A weighted TSA score is calculated, which is estimated from five attributes, namely: weight, space, safety, life cycle cost and operational experience. The results of the case study show that SMES has the lowest life cycle cost but has the highest weight and space requirements, thereby giving it the lowest weighted TSA score. Thus, it is unlikely to be a viable solution for the considered application. On the other hand, SCs require the least weight and space and have the second lowest life cycle cost, which gives them the highest weighted TSA score and makes them the most suitable solution for primary frequency control in an OOGP. Note that the results of the case study depends on the inputs (detailed information about the ES technologies) gathered. However, the most important thing is the methodology and the TSA analysis can always be re-run when more accurate inputs are obtained.

1. Introduction

Carbon emission reduction has been a major priority in the last three decades for many countries due to global warming. The emission trading system has been widely adopted in the European Union, which seeks to apply a tax on corporations that exceed their carbon emission allowance [1]. Some economies (such as Norway, Sweden, Finland and France) have taken a more aggressive approach by applying a direct carbon tax. In light of this, many oil producing economies (such as Norway, UK and Netherlands) are trying to decarbonise the petroleum sector [2,3] which is a significant contributor to greenhouse gas emissions. For offshore oil and gas platforms (OOGPs), offshore wind can provide an interesting source of renewable energy. However, due to the intermittent nature of wind power and high levels of energy security required by oil and gas

Abbreviations: DFIM, Doubly fed induction machine; ELDC, Electrostatic double layer capacitor; ES, Energy storage; ESR, Equivalent series resistance; FC, Fuel cell; GT, Gas turbine synchronous generator; HVAC, Heating, ventilation and air-conditioning; LiC, Lithium-ion capacitor; Li-ion, Lithium-ion; LFP, Lithium iron phosphate; LTO, Lithium titanium oxide; NCA, Lithium nickel cobalt aluminium; NaNiCl, Sodium nickel chloride; NaS, Sodium sulphur; OOGP, Offshore oil and gas platform; O&M, Operation and maintenance; SC, Supercapacitor; SMES, Superconducting magnetic energy storage; TSA, Technology suitability assessment; WT, Wind turbine; WPP, Wind power penetration.

* Corresponding author.
E-mail addresses: ayotunde.a.adeyemo@ntnu.no (A.A. Adeyemo), erick.f.alves@ntnu.no (E. Alves), fmarr@equinor.com (F. Marra), dibrandao@ufmg.br (D. Brandao), elisabetta.tedeschi@ntnu.no (E. Tedeschi).

https://doi.org/10.1016/j.est.2023.106643
Received 13 July 2022; Received in revised form 2 January 2023; Accepted 5 January 2023
Available online 14 February 2023

operations, the use of energy storage (ES) might be inevitable. Additionally, ES can provide other advantages in terms of various power quality improvements [4].

The power system of many platforms is an isolated grid where power is produced locally by gas turbines or diesel generators and characterised by low inertia and limited voltage regulation. Thus, power quality is usually poor in OOGP [5–8]. If intermittent renewable energy sources are integrated into such systems and gas turbines are allowed to shut down, voltage regulation capability and inertia become even lower, and the power quality will worsen. The low system inertia implies that there is a limit to how much wind power can be integrated without jeopardising the system frequency stability in accordance with IEC 61892–1: 2019 [9] and NORSOK E-001:2016 [10] standards. In general, the power consumption in an OOGP ranges between 20 and 100 MW. High-power ES systems with power capacity in the Multi-MW range and low ES capacity (typically in tens of kWh [11]) can be deployed in a wind powered OOGP to provide inertia and primary frequency control, in order to facilitate higher wind power penetration (WPP) levels. ES technologies such as flywheels, SCs and SMES can react faster than gas turbines to loss of load, WTs power fluctuations, and sudden voltage dips. For loss of load and WTs power fluctuation ES can react faster because gas turbines ramp rate is limited by the dynamics of the gas supply, thermal generation system and mechanical system through valves whereas these ES technologies, besides being technology dependent, rely on the dynamics of the power electronic conversion system which has a very short response time and can support high ramp rate. These high-power ES systems can provide services that require rapid high-power charge/discharge such as synthetic inertia and primary frequency control [11–14] and faster voltage support compared to the slower excitation system of the gas turbine synchronous generators (GTs). In particular, a high-power ES can be sized to aid the start of direct on line motors, damp GT rotor oscillation and smooth power oscillations from renewable sources [15–17]. Also, high-energy ES can be sized together with high-power ES in a hybrid configuration to provide secondary frequency control.

However, very few works in the literature have considered the use of ES in an OOGP due to the limited footprint and weight allowance in OOGPs. The authors in [11] developed an analytical approach to size ES for inertia and primary frequency control in an OOGP isolated grid but did not discuss the choice of technology to be used. Likewise, authors in [4,18] proposed ES for power quality improvement but did not discuss the choice of ES. The authors in [19] proposed a battery ES system for increasing the WPP level without elaborating on the technical background of the choice or considering possible alternatives. Lastly, the authors in [20] considered the use of hydrogen storage for reducing carbon emissions in an OOGP, but they reached a technical limit whereby the carbon emissions reduction was limited to a maximum of 36 %. The low roundtrip efficiency of the hydrogen fuel cell (FC) could contribute to the limited carbon emissions reduction. To the best of the authors' knowledge, a technology suitability assessment (TSA) methodology considering the unique harsh conditions of the offshore/marine environment has not yet been proposed in the literature. On the other hand, the authors in [21] assessed the TSA of high-power ES for various applications, but their work did not address the specific requirements (space and weight limits, extreme safety, long life span, low maintenance requirements, etc.) of the offshore environment of OOGPs.

To provide a solid ground for the TSA, it is important to review the latest improvements in ES technologies (not captured by previous works on state-of-the-art of ES technologies) in order to choose an ES with a very high gravimetric and volumetric power density, thereby limiting the weight and space required as OOGPs have highly constrained weight and space. Also, given the extremely cold temperatures in the selected OOGP, there is need to assess ES suitability for operation in these conditions. For example, most batteries tend to have limited capacity and operability in freezing conditions. Although the ES can be placed in a container with heating, ventilation and air-conditioning (HVAC), this will lead to lower overall efficiency and increased operational cost, which needs to be taken into account. Likewise, there is need to select an ES that is very safe considering the highly flammable environment where it has to be deployed. Also, notably, access to OOGPs is usually limited and maintenance and replacement operations are highly discouraged. Thus, an ES with little or no requirement for maintenance and that can last for 20 years should be prioritised. These are some of the factors that need to be considered during TSA of high-power ES. This work seeks to evaluate all the necessary factors and weigh them technically to make the most informed decision for ES selection. Thus, this work performs a TSA of different high-power ES technologies for rapid high-power charge/discharge applications in the OOGP.

The following are the main contributions of this paper:

- Elaboration of a methodology for TSA of high-power ES for application in marine/offshore environment
- Up-to-date information on the current state of the art of consolidated and emerging ES technologies including quantitative parameters.
- Overview of applications of SCs, flywheels, SMES and Li-ion batteries in the offshore and onshore environments.
- Application of the proposed TSA methodology to a real case study of ES deployment in an OOGP for primary frequency control.

The structure of this paper is as follows: Section 2 presents the TSA procedure. Section 3 describes the typical grid services that can be offered by high-power ES. Section 4 presents a case study with ES sizing, weight and space estimation and life cycle cost analysis. Section 5 gathers information on an emerging ES technology, i.e. Lithium-ion Capacitor (LiC), and discusses its suitability for the target application. Finally, section 6 draws the conclusion.

2. Technology suitability assessment procedure

In this section, a systematic approach to assess the suitability of different ES technologies for high-power charge/discharge in OOGP is presented. It is composed of seven steps: the first step is the identification of the required grid service to be offered by the ES. The flow chart for the TSA procedure is shown in Fig. 1.

2.1. Step 1: Identify required grid service

The grid service to be offered is identified. This grid service is used to determine the application requirements in step 2.

2.2. Step 2: Select potential ES candidates from a preliminary list of ES options based on defined application requirements

In this step, the specific application requirements that the potential ES technologies must satisfy are defined. The application requirements are determined by the grid service that the ES has to provide. This step is done in parallel to the preliminary identification of potential ES technology candidates.

2.2.1. Application requirements

Examples of relevant application requirements are:

Number of cycles per day: The number of cycles per day of the application is needed to determine the minimum cycle life needed for the ES. This is particularly important for technologies having relatively low cycle life, such as Li-ion batteries.

Fast response: The required speed of response imposed to the storage by the application must be assessed. This can be a demanding requirement if services such as inertia emulation must be provided.

High pulse discharge: High pulse discharge is when high maximum power is required for a short time but the average power demand is very low. If the application requires high pulse discharges, the ES system that can provide this high pulse discharge with little or no degradation

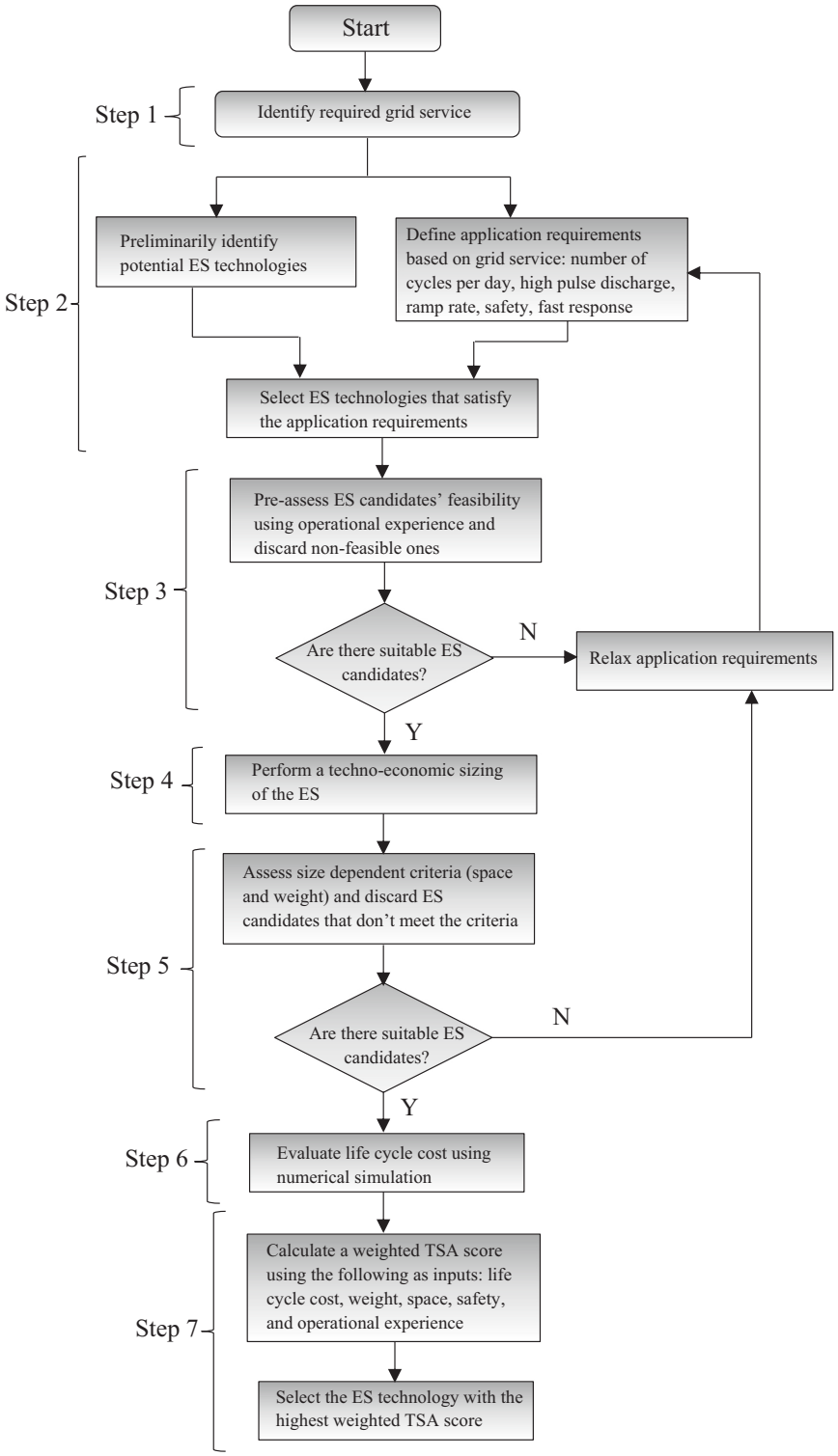

Fig. 1. Flow chart of the technology suitability assessment procedure.

should be prioritised. Oversizing can be considered to limit ES degradation (if Li-ion batteries are used) when high pulse discharge is required.

Ramp rate: If the application requires high ramp rate, an ES that can increase power rapidly needs to be used. For instance, one unit of Beacon power flywheel (with rated power of 300 kW) is able to increase power at 1000 MW/min [22] compared to the gas turbine GE LM2500 GT-SG (with rated power of 20 MW) ramp rate of 20 MW/min [23] and this could help improve frequency regulation.

Safety: The ES safety requirement of the application needs to be assessed. For example, due to the highly flammable nature of an OOGP, risk of fire such as thermal runaway in some Li-ion chemistries cannot be tolerated.

2.2.2. *Identify potential ES technologies*

An initial list of potential ES technologies is drawn. The ES

technologies in this list are assessed against the given application requirements to preliminarily check their suitability. ES technologies that meet the application requirements are investigated further.

2.3. Step 3: Selection of potential ES technologies using operational experiences

From the list of ES technologies that satisfy the application requirements, a further selection of suitable ES for the target application is performed based on operational experiences of the ES technologies in practical deployment. The ES technologies that meet the application requirements and have good operational experiences in proximal fields are analysed further as potential ES solutions. If there are no suitable ES candidates the application requirements in step 2 have to be relaxed and the process is started again from step 2.

After the candidate ES technologies have been identified within a broader pool based on the application requirements and operational experiences, the size of the required ES system is estimated.

2.4. Step 4: Techno-economic sizing of the ES

The power and energy ratings of the ES are sized to be able to determine the space and weight that will be required for ES deployment and also to determine the life cycle cost of operating the ES. The sizing of the ES is an intricate task, and this stage may not always be finalised in the TSA. Nevertheless, the suitability of the ES for a given application should still be assessable even without accurate knowledge of the ES size. The techno-economic sizing relies on simulation of the power system, and this is exemplified using a case study in section 4.4.

2.5. Step 5: Evaluate ES size-dependent application constraints

Once the size of the potential ES is assessed, the two critical criteria that depend on ES rating and must be met are then assessed, i.e.:

- *Space*: Due to limited space on OOGPs, the ES must have high volumetric power density (kW/L). This is not just limited to volumetric power density of the ES but to the actual footprint of all the ES components (including necessary auxiliary systems), which cannot exceed a certain value. For example, for flywheel the space required should include the space for the flywheel system with the housing, the power electronic module and the cooling system. Likewise for other ES technologies the space required should include the space for power electronic module, the HVAC and other necessary components.
- *Weight*: Also, due to limited allowable weight on OOGPs, the ES must have high gravimetric power density (kW/kg). This is also not limited to the gravimetric power density of the ES, but it also includes the overall gravimetric power density of the ES and its balance of plant.

If there are no suitable ES technologies after the ES have been pre-screened with weight and space limits, the application requirements in step 2 are relaxed and the process is started again from step 2.

2.6. Step 6: ES life cycle cost assessment

After the potential ES technologies have been pre-screened based on application requirements, operational experience and weight and space constraints, the life cycle cost of the ES technologies is evaluated. The ES size obtained in step 4 is used to evaluate the life cycle cost.

2.7. Step 7: Decision making on the most suitable ES technology using a weighted TSA score

After the ES life cycle cost has been determined, a weighted TSA score is calculated and the ES with the highest weighted TSA score is chosen. The attributes that are scored include the following: life cycle cost, weight, space, safety and operational experience. This weighted TSA score is calculated and explained in the case study in section 4.7.

3. Typical grid services provided by high-power energy storage

Before presenting the application of the proposed TSA procedure to the considered test case, typical grid services provided by ES systems are reviewed to lay the foundation for the first step of the procedure.

3.1. Inertia emulation and primary frequency control

Inertia emulation and primary frequency control are frequency regulation grid services where power reserves are deployed to balance the mismatch between generation and load in order to maintain frequency at or close to the nominal value. Inertia emulation helps to increase the equivalent system inertia thereby limiting the rate of change of frequency while primary frequency control helps to limit the steady state frequency deviation. When generation exceeds load, the frequency increases above rated value and when load is higher than generation, the frequency drops below rated value. According to the NORSOK standard [10], in an OOGP, frequency has to be regulated within ±10 % for transient operation and ±5 % for continuous operation. Also, GTs have a maximum ramp rate that must not be exceeded. High-power ES can be used during transient events to keep the GTs well below the hard limit while the ES provides active power until the GTs are able to take over and restore the frequency of the OOGP grid to the rated value.

ES has been deployed for primary frequency regulation service in national grids [24,25] and can similarly be deployed in an OOGP to improve frequency regulation. Operational experience of the use of flywheels in an island for primary frequency regulation to allow higher WPP is detailed in [26]. ES was also used in [4] to improve the frequency regulation of an OOGP grid during transient events.

3.2. Voltage support

Voltage support is one of the grid services where ES or generators inject or absorb reactive power in order to maintain the grid voltage close to the rated value. In an OOGP, grid voltage at the point of common coupling must be maintained at ±20 % for transient operation and +6 %/−10 % for continuous operation [10]. High-power ES devices can also be sized to provide voltage support during transient events such as during the start of a direct on line induction motor. Using ES will help achieve much better voltage regulation as the ES converter can react much faster than the excitation system of GTs. This is particularly attractive for OOGP because most of the loads are constituted by large motors. The authors in [4] sized ES for frequency and voltage support, but the voltage support capability is limited by reactive power allocation of the ES converter when concurrently supplying rated active power. However, the economic value of sizing the ES converter to provide reactive power as well as active power needs to be assessed. In line with this, the authors in [18] proposed a dynamic converter capacity allocation for voltage support, harmonic and unbalance power compensation to maximise the cost-benefit of the ES system. Another alternative that can be explored in an OOGP is the cooperative control of pre-existing voltage source converters in the system for voltage regulation service during transient events.

3.3. Voltage sag mitigation and fault-ride through

Voltage sag is a temporary drop in the voltage due to load unbalance or faults in the power system. A voltage sag occurs when a load draws a large amount of power for a short period of time. Voltage sags can lead to voltages dropping to any value, typically between 10 % and 90 % of

nominal value. Most voltage sags usually last between 20 ms – 50 ms [27]. Short-circuit faults in the power system can also cause voltage sags. High power ES has been deployed to mitigate voltage sags as it can quickly sense the drop in voltage and supply reactive power to maintain the voltage at rated values [28–30].

3.4. Low frequency oscillation damping

Low frequency GT rotor oscillations are common in isolated power system with low inertia [31]. This low frequency oscillation can typically be in the range 0.1–2 Hz [31]. This becomes even worse when WTs are integrated [32], which results in low inertia if one GT is shut down for higher WPP. Also, wide fluctuations in the wind speed can transfer to the rotor of the GT. The common way to damp low frequency oscillations is the use of damper bars on the GT rotor windings, but this leads to significant losses. High-power ES can be used to mitigate this low frequency oscillation of the GT rotor by absorbing or injecting real oscillatory power with very little power loss. The high-power ES systems (flywheels, SCs and SMES) have very fast response (10 ms or less) that make them suitable for this application.

3.5. Power smoothing

The wind power from a WT is directly proportional to the cube of the wind speed. Thus, high frequency fluctuations in the wind speed can cause a significant disturbance in the local power system. These fluctuations in wind speed (particularly the high frequency ones) lead to continual ramping up and down of the GT by the action of the governor. There are regulations for connected renewables particularly in interconnected systems. For example, in China, renewable power fluctuation must be limited to 10 % of rated capacity per minute in order to guaranty stability of the power system [33]. Similarly, renewable power fluctuation for an OOGP must be limited. Furthermore, operating the GT in this manner will lead to its accelerated wear and tear. It is very desirable to smoothen the power supplied by the WTs to guarantee safe and reliable operation and better power quality on the OOGP power system. Several works [34–36] have sized high-power ES for smoothing the power output of WTs integrated to the grid. The methods used in these works can be applied for power smoothing in an OOGP.

3.6. Increasing renewable penetration in isolated grids/islands

Several factors contribute to the curtailment of renewable energy in isolated grids on islands and in remote communities where grid inertia is low. They include the spinning reserve requirements, which are necessary to guarantee reliability of power supply. Thus, it is common to have diesel generators or GTs running at low load to provide this spinning reserve, which is uneconomical. Also, diesel generators and GTs usually have maximum ramp rates and limited ability to respond quickly to large step load changes. Thus, it is common to have more generation capacity online to allow better dynamic response (i.e., better voltage and frequency regulation) to step load changes. This is also uneconomical. Additionally, diesel generators and GTs usually have minimum load requirements, which means that renewable power above certain limits must be curtailed. Furthermore, stringent voltage control requirements and power system stability limit the amount of power fluctuations the power system can accommodate, which ultimately leads to curtailment of renewable power. However, high-power ES can be integrated with low inertia system for stabilisation of the grid frequency and voltage, thereby facilitating higher renewable penetration. A number of projects [37–41] have already deployed some high-power ES systems for this purpose, which are discussed in section 4.3.

4. Case study

4.1. OOGP configuration

In this work, three OOGP configurations are briefly described but only one configuration is used to exemplify the TSA procedure described in section 2. The OOGP grid in configuration 1 has GT and loads but no ES or WT. This corresponds to most OOGPs currently in use. Configuration 2 shows the OOGP grid with GT, loads and ES but no WT. Configuration 3 shows the OOGP grid with GT, loads, ES and WT, and is considered as a further future development for OOGP. The three configurations are shown in Fig. 2.

In this section, a case study based on OOGP configuration 2 is presented that uses the TSA procedure described in section 2 to select the best ES technology. Among the various relevant alternatives presented in Section 3, the grid service considered in this case study (step 1) is primary frequency control. In practice, an ES will be deployed to deliver multiple services as this is more economical, but for the sake of illustrating the TSA procedure presented in section 2, only one grid service has been considered.

4.2. Test case description

The case study is based on a real OOGP platform in the North Sea. The platform has four GE LM2500 gas turbines each with a power rating of 20.2 MW/25.25 MVA. Detailed information on the GTs is given in Appendix B. A single-line diagram of the platform is shown in Fig. 3. According to NORSOK standards, the transient frequency deviation on an OOGP is allowed to vary within ±10 % of the rated value [10]. The current study aims for a maximum frequency deviation of ±5 %. The NORSOK standard is a hard technical limit and for best performance, the platform grid should not be operated close to the limit. Besides, most machines and transformers are not designed to operate at a frequency deviation higher than 5 %.

4.3. High-power energy storage (step 2)

4.3.1. Selection of potential ES candidates based on application requirements

The TSA procedure proceeds in step 2 which, based on the definition of the grid service in step 1, establishes the consequent application requirements and selects the potential ES candidates from a preliminary list. Among the possible application requirements introduced in Section 2, primary frequency control does not require a fast response, since inertia emulation is not considered, but requires a high ramp rate. From the one-year load profile corresponding to the case study, there were 1348 occasions when the change in load caused a frequency deviation larger than the dead band (±0.25 %), at which point the ES provides power. The load profile and the simulation model for frequency response are presented in section 4.4.2, but this preliminary assessment shows that this service may demand close to 3.7 full cycles per day (it is likely less because for small load changes the full capacity of the ES will not be used), which implies that an ES with a high cycle life (26,960 cycles for a 20-year project life) is needed. The small deadband increases the ES usage (as seen from the required cycle life) but this reduces frequency oscillations and increases the frequency stability of the low-inertia isolated power system. This service can also be characterised as high pulse discharge, as the instantaneous power required during the delivery of this service is high compared to the average power to be delivered. This necessitates an ES with high power density. Also, given the highly flammable nature of the OOGP environment, high safety is required from the ES.

The preliminary list of ES choices included SCs, flywheels, SMES, Li-ion batteries, sodium nickel chloride battery (NaNiCl), sodium sulphur battery (NaS) and nickel cadmium battery (Ni—Cd). SCs, flywheels and SMES are generally known to have high power density, but battery

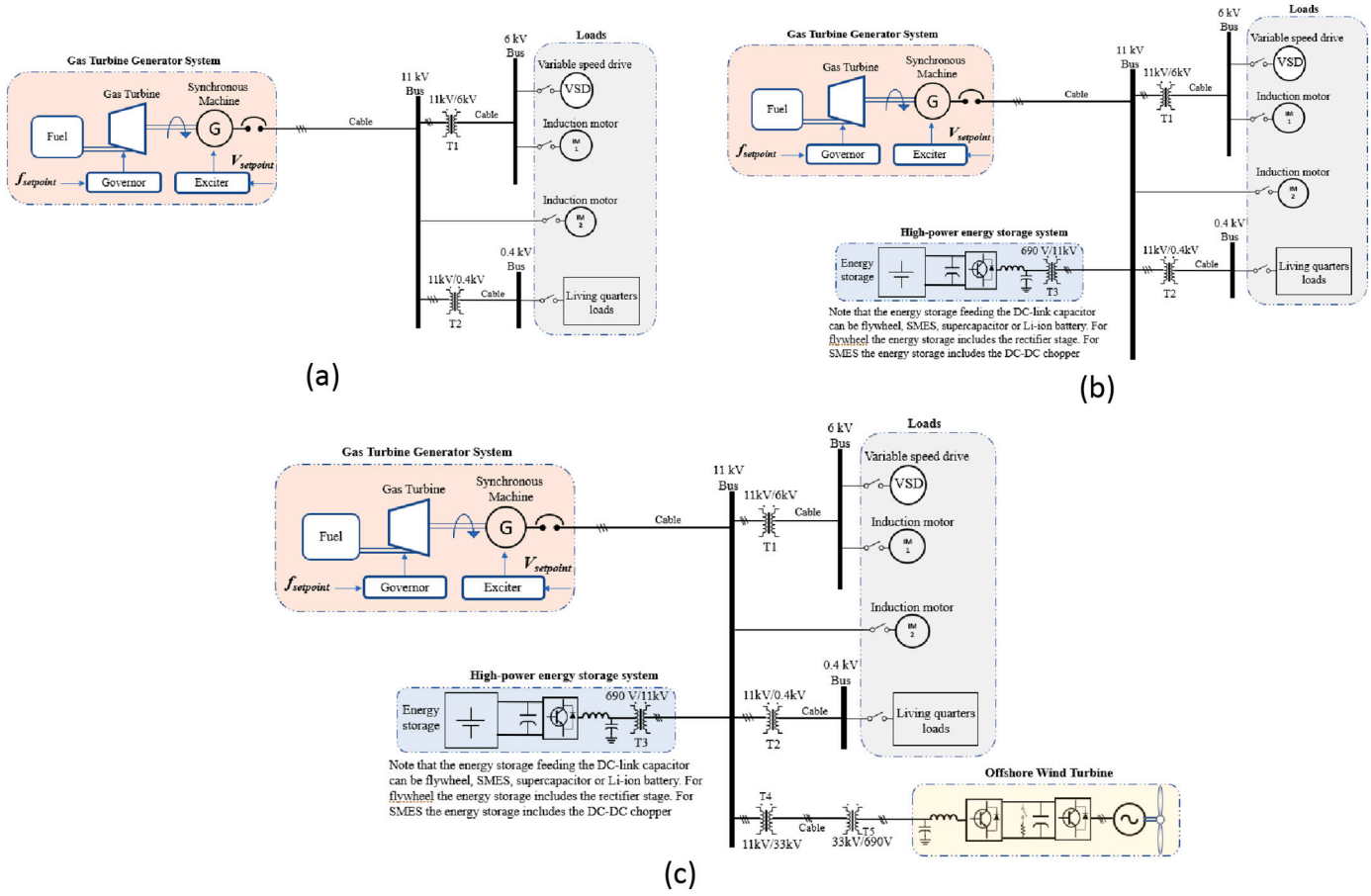

Fig. 2. (a) OOGP Configuration 1 (b) OOGP Configuration 2 (c) OOGP Configuration 3.

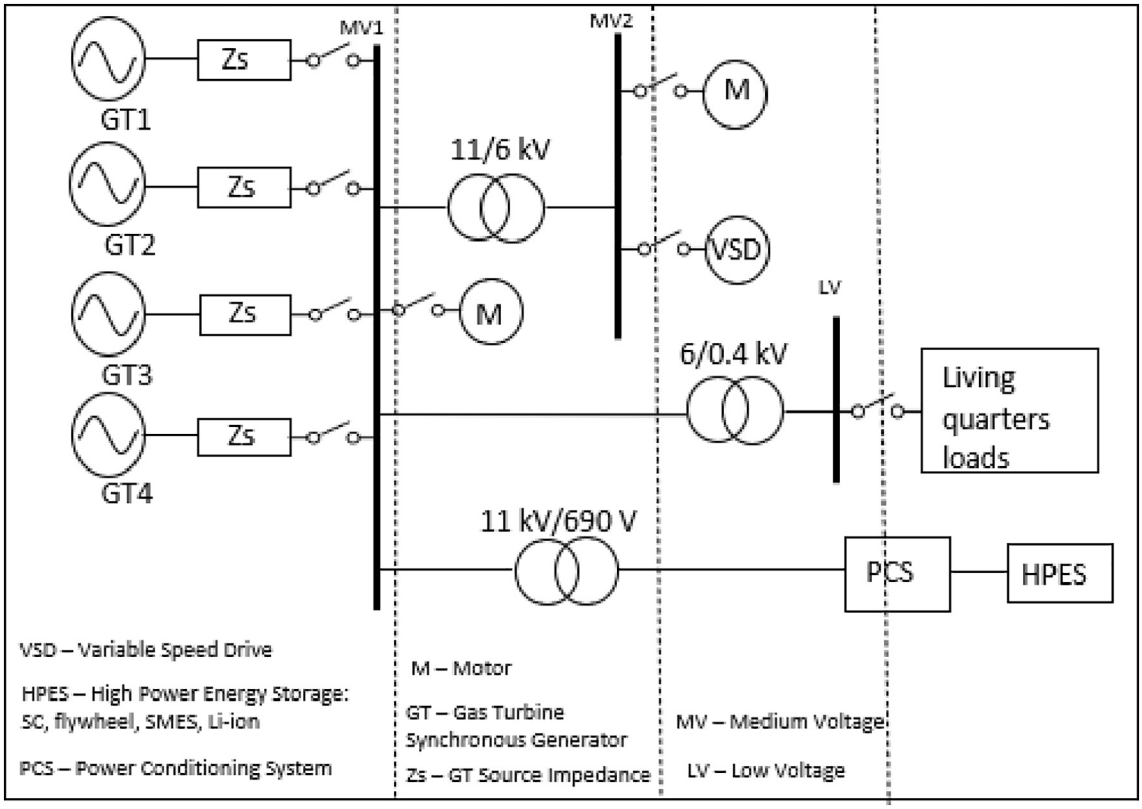

Fig. 3. Single-line diagram of the case study platform.

Table 1
Comparison of the power density and cycle life of the considered battery chemistries.

	Power density (W/kg)	Power density (W/L)	Cycle life
Li-ion	150–500 [21]	400–2000 [21]	1500–10,000 [21]
NaS	150–230 [42]	–	2500–4500 [43]
NaNiCl	150–200 [42]	220–300 [42]	2500–3000 [42]
Ni-Cd	150–300 [42]	–	2000–2500 [42]

technologies have much lower power density. Table 1 shows the volumetric power density, gravimetric power density and cycle life of the considered battery technologies. It can be seen from Table 1 that Li-ion has higher power density and cycle life (up to 10,000 if lithium iron phosphate (LFP) is used) compared to the other battery chemistries and it is therefore the major contender for use in this case study among the considered battery chemistries.

Table 2 shows the seven ES technologies and the application requirements they do or do not satisfy. NaNiCl battery does not satisfy the requirement for high power density and high cycle life. NaS battery does not satisfy high power density, while Ni—Cd does not satisfy high cycle life and high power density. From the preliminary list, only SCs, flywheels, SMES and Li-ion batteries satisfy all the application requirements and are deemed suitable for the targeted service in agreement with the previous literature [21,28]. Thus, NaNiCl, NaS and Ni—Cd are discarded and are no longer considered in this work.

The outcome of Table 2 is derived as follows: For cycle life the requirement is 26,960 cycles and SC, SMES and flywheel can each do at least 100,000 cycles. NaS and Li-ion can also satisfy this requirement if they are oversized. For high power density, it is well established that SCs, flywheels and SMES have some of the highest power densities, thus their inclusion in the analysis is straightforward. But batteries are not known for high power density. However, Li-ion have high power density and the highest power density among batteries as shown in Table 1 and have been considered for high power applications in [21,28]. Thus, Li-ion is chosen to satisfy this requirement. It is well established that all the ES technologies have high ramp rate. For safety, SC, SMES and NiCd are known to be inherently safe. Flywheels are usually built with containment housing as a safety mechanism in case the flywheel fails and are also considered safe. Li-ion batteries are well known to have risk of thermal runaway. But there are two Li-ion chemistries that are very safe, which are LFP and lithium titanium oxide (LTO). Additionally, a robust battery management system can be equipped with Li-ion batteries to ensure that the risk of thermal run away is eliminated through

Table 2
Application requirements for primary frequency control.

Application requirements	SC	SMES	Li-ion	Flywheel	NaNiCl	NaS	NiCd
High cycle life	✓	✓	✓	✓	×	✓	×
High power density	✓	✓	✓	✓	×	×	×
High ramp rate	✓	✓	✓	✓	✓	✓	✓
High safety	✓	✓	✓	✓	✓	✓	✓

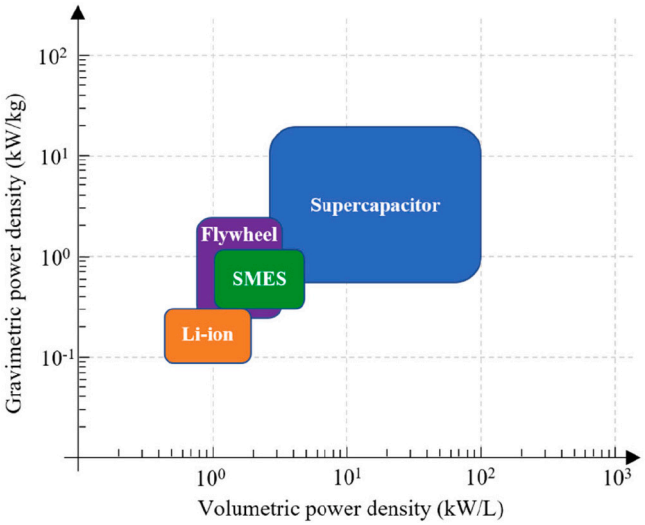

Fig. 4. Range of power density of high-power energy storage technologies.

robust cell monitoring and the ability to disconnect faulty cells. In fact, Li-ion battery has already been installed on an OOGP off the coast of Australia (Goodwyn A platform). Thus, Li-ion is also certified safe. NaS and NaNiCl are also certified safe as the risk of molten sodium burning in air is eliminated through complex manufacturing procedure.

It should be noted that the selection of suitable ES may be different if a different grid service is considered, which will imply different application requirements. The state-of-the-art of SCs, flywheels, SMES and Li-ion batteries including up-to-date manufacturers' data is reviewed in detail in Appendix A. The main task is to evaluate these ES technologies to determine which one is most suitable for an OOGP considering the harsh operating conditions and additional constraints imposed by the offshore environment.

4.3.2. *Comparative analysis among the four ES technologies (step 2)*

Fig. 4 shows the range of gravimetric power density and volumetric power density for the four ES technologies. Table 3 presents the characteristics of the four high power ES technologies. Fig. 5 visually compares the roundtrip efficiency, self-discharge rate, life span and life cycle of the four assessed ES technologies. Li-ion batteries have lower power density than flywheels, SCs and SMES, but it is their relatively short cycle life that is the major drawback as the rapid high-power applications they are to be used for can demand very frequent charge/discharge cycles. Flywheels, SCs and SMES have better performance in this respect, as they can do at least 100,000 cycles; much better than the maximum of 10,000 cycles possible for the best Li-ion batteries [21]. One way to overcome this is to oversize the Li-ion battery, which will enable it to deliver the required cycle life.

Even though flywheels have a lower cost per kWh compared to SMES and SCs, they may not be the best solution due to their prohibitively high self-discharge losses in the flywheel drive, motor/generator (core loss

Table 3
ES Technology attributes.

Item	Supercapacitor	SMES	Li-ion battery	Flywheel
Gravimetric Power density (kW/kg)	1–10 [21]	0.5–2 [21]	0.15–0.5 [21]	0.5–4 [21]
Volumetric Power density (MW/m^3)	0.4–10 [21]	1–4 [21]	0.4–2 [21]	1–2.5 [21]
Gravimetric Energy density (Wh/kg)	0.5–5 [21]	1–10 [21]	70–200 [21]	10–50 [21]
Volumetric Energy density (kWh/m^3)	4–10 [21]	0.2–2.5 [21]	200–600 [21]	20–100 [21]
Response Timescale (ms)	2 ms [50]	1 ms	3–5 ms [51]	10 ms
Discharge time	Milliseconds – 5 mins [21]	Milliseconds – 8 s [42]	Mins – hours [42]	Milliseconds - 15 mins [42]
Cost per kWh ($)	500–15,000 [28]	1000–10,000 [28]	240–2500 [28]	2000–5000 [21]
Cost per kW ($)	100–400 [28]	200–500 [28]	686–4000 [28]	150–400 [28]
Operating temp. (°C)	−40 to 65 [21]	−50 to 60 [21]	−20 to 65 [21]	−40 to 40 [21]

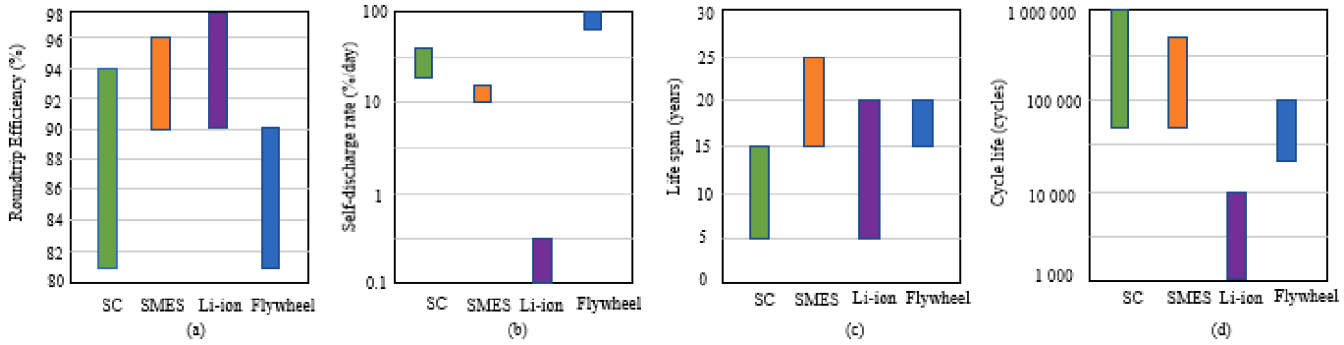

Fig. 5. (a) Roundtrip efficiency (b) Self-discharge rate (c) Life span (d) Cycle life of high-power ES.

and copper loss) and power electronic converter [44–49]. However, one advantage with flywheels is that HVAC is generally not required in most flywheel designs as flywheels can operate under a wide temperature range. A simple water-cooling system is sufficient for most flywheel designs. For low C-rate (which indicates how much current a battery is able to deliver for a given Ah rating; for example, a 2 Ah battery with a C-rate of 0.5C can deliver 1 A) flywheels the standby/idling losses (all the losses in the flywheel system including power electronics) should be similar to power supplied to the HVAC of an equivalent Li-ion battery. But for high C-rate flywheel the idling losses are significantly more than the power supplied to the HVAC of an equivalent Li-ion battery. Since most flywheels design are high C-rate the standby losses must be taken into consideration when performing TSA of ES technologies.

Losses in the flywheel drive include the losses in the bearing (if active magnetic bearing is used) and windage losses. The losses due to the bearing are estimated to be 5 % of rated energy per hour for mechanical bearings, 1 % for electromagnetic bearing and can be reduced to 0.1 % for high temperature superconductor (HTS) bearings [44]. While modern flywheels are mounted in a vacuum to reduce windage losses and with the development in recent years particularly in low loss bearings such as active magnetic bearings and HTS bearings to further reduce losses [44,52], the idling losses in flywheel are still higher than the ancillary loads of other ES technologies particularly when used for high C-rate applications due to other non-windage losses. For high C-rate applications such as the one considered in this work, the idling loss will be high because a large motor/generator is connected to a flywheel of small rated energy. In this case, a high percentage of the idling losses will be in the motor/generator.

The major advantage of SMES is its high power density which enables it to easily scale up to tens of MW or even hundreds of MW from small energy storage unit [53]. The drawbacks of SMES are its low energy density and short discharge time in comparison to flywheels and SCs, which leads to a requirement for more space. Note that Multi-MW ES are also achievable with SC, flywheels and Li-ion but this requires connecting multiple units together which may lead to sub-optimal space use particularly for flywheels. More technical evaluations are needed to determine the best ES to use, which are presented in the following sections.

4.4. Proposals and operational experience of high-power ES deployment in the offshore/marine environment (step 3)

This section primarily reviews works on ES solutions for application in the offshore/marine environment. Where reported operational experience of practical deployment of high-power ES technologies in offshore/marine environment is lacking, proposals/simulation studies for marine applications and operational experience in non-offshore environment are included. Since this work targets Multi-MW ES in isolated OOGP, the knowledge that these ES technologies have been deployed in the power range of the target application is a preliminary indication of feasibility. Table 4 shows the ES proposals and operational experience.

Most of the operational experience of supercapacitor deployment is in the transportation sector. The authors in [54,55] review some of the applications of SCs in electric vehicles and trains for regenerative braking. The high-power density and high efficiency of SCs make them the ideal choice for electric transportation where space is at a premium and little ES capacity is required. SCs are not usually considered for grid applications due to their low energy density, relatively short life span and high cost. However, several authors have proposed using SCs for power smoothing of wave energy converters [16,17,56–59] or for mitigating high power disturbances in a ship electrical system [60–63]. The major caveat is that SCs are mostly used for applications in the kW range although there are examples of multi-MW application of SCs [28].

Most of the operational experience of SMES is for voltage support and voltage sag mitigation. This is because SMES has a low energy density which makes it less suitable for frequency regulation services where significant active power is required. Nevertheless, SMES was used in [64] (Table 4) for frequency regulation which indicates that SMES can be considered.

While Li-ion batteries can be designed to run for hours, this is not the scope of application being considered in this work as this work considers applications with short discharge time. Since the grid service considered in this work has a rather short discharge time, the C-rate of the Li-ion battery will need to be high. In fact, most of the Li-ion applications listed in Table 4 have a high C-rate ($\geq$2C). For example, the deployments in Li-ion/Laurel Mountain, West Virginia [65] and Li-ion/New York [66] in Table 4 have C-rate of 4C and 8C respectively. In addition to high C-rate, if Li-ion will be used, it will still likely be oversized to be able to provide the needed power, as an excessively high C-rate can lead to fast degradation of the battery.

One of the proven operational experiences of flywheels is their use for grid voltage and frequency stabilisation in isolated power systems with low inertia and high renewable penetration. Operational experiences listed in Table 4 show that flywheels can be used for improving the voltage and frequency regulation and increasing WPP level in the isolated grid of an OOGP. However, despite advancement in flywheels, flywheels still consume high power to keep spinning when not in use (standby/idling losses) and these losses can be significant over a period of a year. So, it is good to weigh these operational losses against the gains and in comparison with other high power ES choices from a life cycle cost analysis perspective to determine the most suitable ES choice, assuming critical factors such as safety and weight/space constraints are satisfied. This is addressed in section 4.6.

Table 5 shows the various operational experience criteria satisfied by the ES technologies.

Based on the considerations regarding pre-existing operational experiences, as summarised in Table 5, all four ES technologies are

Table 4
High-power ES proposals and operational experience.

ES technology/location	Environment	Rating	Application	Type
Supercapacitor [15]	Offshore	16 kW	Power smoothing of wave energy converter	Simulation studies
Supercapacitor/China [28]	Non-offshore	3 MW/17.2 kWh	Voltage sag mitigation	Deployed (2011)
Supercapacitor/Spain [28]	Non-offshore	4 MW/5.6 kWh	Frequency stability	Deployed (2013)
Supercapacitor [63]	Offshore	194 kW/2.05 Wh	Mitigation of power fluctuation in electrical ship propulsion	Simulation studies
Supercapacitor [67]	Offshore	50 kW/300 Wh	Power smoothing of marine current turbine	Prototype
SMES [29]	Non-offshore	1.4 MVA/0.67 kWh	Voltage sag mitigation and fault ride-through	Operational experience
SMES/Chubu Electric power co., Japan [30]	Non-offshore	10 MW/5.86 kWh	For mitigating instantaneous voltage sag	Deployed
SMES/Upper Wisconsin, USA [64]	Non-offshore	3 MW/0.83 kWh, 8 MVAR	Frequency regulation and reactive power supply	Deployed (2000)
SMES [68]	Non-offshore	5 MVA/2.04 kWh	Voltage support	Deployed (2003)
SMES/Nosoo Power station, Japan [69]	Non-offshore	10 MW	Power quality and power stability improvement	Deployed
Li-ion/Laurel Mountain, West Virginia, USA [65]	Non-offshore	32 MW/8 MWh	Frequency regulation	Deployed (2011)
Li-ion/New York, USA [66]	Non-offshore	16 MW/2 MWh	Frequency regulation	Deployed (2011)
Li-ion/Tohoku, Japan [66]	Non-offshore	40 MW/20 MWh	Aid renewable integration	Deployed (2013)
Li-ion/Carrickfergus, UK [70]	Non-offshore	10 MW/5 MWh	Frequency regulation	Deployed (2016)
Li-ion/Leighton Buzzard, UK [70]	Non-offshore	6 MW/10 MWh	Frequency regulation	Deployed (2014)
Li-ion/Rise Carr, UK [70]	Non-offshore	2.5 MW/5 MWh	Voltage support	Deployed (2014)
Li-ion/Wolverhampton, UK [70]	Non-offshore	2 MW/1 MWh	Frequency regulation	Deployed (2014)
Flywheel/USA [24]	Non-offshore	20 MW	Frequency regulation	Deployed (2013)
Flywheel/New York, USA [25]	Non-offshore	20 MW	Frequency regulation	Deployed (2011)
Flywheel [26]	Non-offshore	500 kW/5 kWh	Frequency regulation for increased renewable penetration	Operational experience
Flywheel/Kalbarri, Western Australia [37]	Non-offshore	1 MW	Flywheel deployed as a STATCOM to support grid connection of WTs	Deployed (2008)
Flywheel/Marsabit, Kenya [37,39]	Non-offshore	500 kW/5 kWh	Grid voltage and frequency stabilisation and enable higher WPP	Deployed (2016)
Flywheel/Kodiak Island, Alaska [37,40]	Non-offshore	2 × (1 MW)	Grid voltage and frequency stabilisation and enable higher WPP	Deployed (2015)
Flywheel/UK [71]	Non-offshore	2 × (400 MW/720 kWh)	High power supply to nuclear fusion furnace	Operational experience
Flywheel [72]	Offshore	1 MW/25 kWh	"black" start on an All-Electric ship	Proposal
Flywheel [73]	Offshore	100 MW	Fault-ride through enhancement	Simulation studies
Flywheel [74]	Offshore	1 MW/8.3 kWh	Voltage support for motor start	Simulation studies
Flywheel/Utsira-Norway [75]	Non-offshore	200 kW/5 kWh	Power smoothing of wind energy	Operational experience
Flywheel/Coral Bay, Australia [76]	Non-offshore	500 kW/5 kWh	Power smoothing of wind energy	Deployed (2007)

Table 5
Operational experience criteria of the ES technologies.

ES technology	SC	SMES	Li-ion	Flywheel
Proven application with required power and energy rating	✓	✓	✓	✓
Previously used for primary frequency control	✓	✓	✓	✓
Previously used in isolated power systems	✓	✓	✓	✓
Previously used in grid applications	✓	✓	✓	✓

considered potentially viable for the intended application and included in the following analysis. There is a lack of application in offshore/marine environment for all four ES technologies, and this is therefore not considered in the selection of the ES system for further investigation. Li-ion batteries have been used in many marine applications, but within the scope of the services considered in this work, there is no report of Li-ion application.

4.5. Techno-economic sizing of the energy storage (step 4)

4.5.1. ES apparent power rating

The primary function of the high-power ES is to provide frequency regulation. Thus, the apparent power of the ES converter will be rated close to its rated active power leaving a margin of 10 %. Thus, reactive power supply that can be provided will depend on the active power demand, although reactive power supply is not a grid service in focus in this case study.

4.5.2. Description of simulation model

In this design, the three parameters that are sized are ES rated power, ES rated energy and damping factor due to the damper windings on the rotor of the GTs. The conventional way to reduce large frequency excursions and damp low frequency oscillations is the use of damper windings. However, this is a very inefficient approach due to losses in the damper windings. The amount of damping provided by the damper windings is limited in this work to reduce losses. The inertia constant of

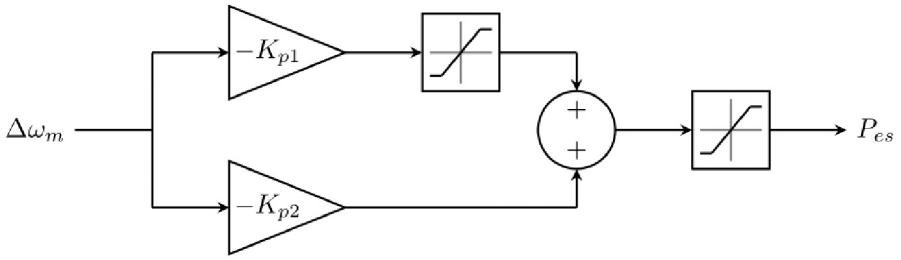

Fig. 6. Control diagram of the ES double-proportional droop control.

the LM2500 is 2.01 s, which is close to that modelled in [4] (1.85 s). This low inertia constant needs a high damping factor as evidenced by the value used in [4] (7.04). In comparison, the model in [11] has a damping factor of 2.25, which is expected because the inertia constant is high (5.1 s). In this model, a damping factor of 1.5 for the damper windings (to reduce losses) is used. With this damping factor, the ES power and energy rating needed to keep the frequency excursion within ±5 % are determined. Through a few simulation runs, the power and energy ratings of the ES system are derived simultaneously. A simplified model based on the swing equation is used to estimate the frequency response of the system as described by Eqs. (1)–(4) [77]. The work of [4] shows that the simplified model gives a result close to that of the detailed model with voltage dynamics, which proves the validity of the simplified model.

$$J \bullet \frac{d^2\theta}{dt^2} = J \bullet \frac{d^2\delta}{dt^2} = T_q = T_m - T_e - T_d \tag{1}$$

$$T_d = k_d \bullet \Delta\omega_m = k_d(\omega_s - \omega_m) \tag{2}$$

$$J \bullet \omega_m \bullet \frac{d^2\delta}{dt^2} = P_q = P_m - P_e - P_d \tag{3}$$

$$\frac{J\omega_m}{S_{base}} \bullet \frac{d^2\delta}{dt^2} = \frac{P_m}{S_{base}} - \frac{P_e}{S_{base}} - \frac{P_d}{S_{base}} = P_m - P_e - P_d \tag{4}$$

where J is the inertia of the GTs, θ is the physical rotor angular position with respect to a fixed axis, δ is the rotor angular position with respect to the position of the synchronously rotating magnetic field, T_q is the accelerating or decelerating torque, T_m is the mechanical torque, T_e is the electrical torque, T_d is the torque provided by the damper windings, $\Delta\omega_m$ is the change in the rotor angular speed, ω_s is the synchronous speed of the machine's magnetic field, ω_m is the rotor angular speed, P_q is the accelerating or decelerating power, P_m is the mechanical power, P_e is the electrical power, P_d is the power provided by the damper windings and S_{base} is the base apparent power.

Eq. (5) gives the inertia constant of the GTs.

$$H = \frac{J \bullet {\omega_s}^2}{2 \bullet S_{base}} \tag{5}$$

By substituting for J in Eq. (4) using Eq. (5) and assuming that in steady state $\omega_s \cong \omega_m$, the expression for the frequency control as a function of the inertia constant and the powers is given in Eq. (6):

$$\frac{d^2\delta}{dt^2} \bullet \frac{2H}{\omega_S} = P_m - P_e - P_d \tag{6}$$

Since high-power ES is added to the system, Eq. (6) becomes Eq. (7):

$$\frac{d^2\delta}{dt^2} \bullet \frac{2H}{\omega_S} = P_m + P_{es} - P_e - P_d \tag{7}$$

where P_{es} is the ES power.

In this case study, a double-proportional droop control is proposed for a faster release of the ES power so as to achieve better frequency control. Eqs. (8)–(11) express the ES power using the double-proportional droop control:

$$P_{es} = \left[K_{p1} \bullet \Delta\omega_m\right] + K_{p2} \bullet \Delta\omega_m \tag{8}$$

$$\left[K_{p1} \bullet \Delta\omega_m\right] \leq \pm\frac{0.5 \bullet P_{es\_nom}}{S_{base}}\ pu \tag{9}$$

$$P_{es} \leq \pm\frac{P_{es\_nom}}{S_{base}}\ pu \tag{10}$$

$$S_{base} = 101\ MVA \tag{11}$$

where K_{p1} and K_{p2} are proportional gains and P_{es_nom} is the ES nominal power. K_{p1} is designed such that the output of $K_{p1} \bullet \Delta\omega_m$ saturates once the frequency deviation reaches ±0.005 pu and the total ES power, P_{es}, saturates once the frequency deviation reaches 0.02 pu. The control system of the double-proportional droop control is shown in Fig. 6. K_{p1} and K_{p2} are designed such that at frequency deviation of ±0.005 pu, P_{es} equals $\pm 0.5 \bullet P_{es\_nom}$ and at frequency deviation of ±0.02 pu, P_{es} equals $\pm P_{es\_nom}$. Each GT on the platform has a base apparent power of 25.25 MVA. Thus, the total apparent power on the platform is 101 MVA, which was chosen as the base apparent power.

Also, it is crucial to note that the GT of model GE LM2500 has a maximum ramp rate of 20 MW/min. Thus, the primary and secondary control of the GT is limited using a rate limiter block. A dynamic rate limiter block in Simulink is used due to the fact that the number of GT running depends on the load. There are times when only two GTs are operating. This rate limiter is used to limit the control action of the secondary control PI controller. When the rate limiter is active, the integral of the secondary control is stopped using an anti-windup block to avoid frequency overshoot. A proportional controller is then used to reduce the error between the input and output of the rate limiter to avoid frequency overshoot. Fig. 7 shows the control system of the Simulink model of the frequency control with ES. The rest of the modeling parameters for the OOGP can be found in Appendix B.

A one-year data with 15-min resolution (35,040 samples) is obtained for the selected platform. A histogram of the platform load demand is shown in Fig. 8. It is assumed that very small load changes happen within two time intervals since most loads on the platform are large motors. This load data is used to simulate the energy exchanged by the ES with the OOGP grid in a year. The use of the load data for computing the exchanged energy with the grid is explained in section 4.6.

Now, the power and energy rating of the ES will be determined through simulation. There is need for information on the largest load on the platform in order to determine the ES rating needed to keep the grid frequency within ±5 %. From the information obtained, the largest load is a 7 MW motor on the platform. Thus, a maximum load change of 7 MW is chosen. For the simulation, it is assumed that the load is 0.2673 pu (27 MW). It is assumed that only 2 GTs are operating since the load is low. This makes it possible to size the ES under the worst case scenario as the reduced inertia and reduced ramp rate leads to the poorest frequency regulation. The system is simulated for a drop in load of 7 MW (0.0693 pu) from 0.2673 pu (27 MW) to 0.198 pu (20 MW). It is assumed that the

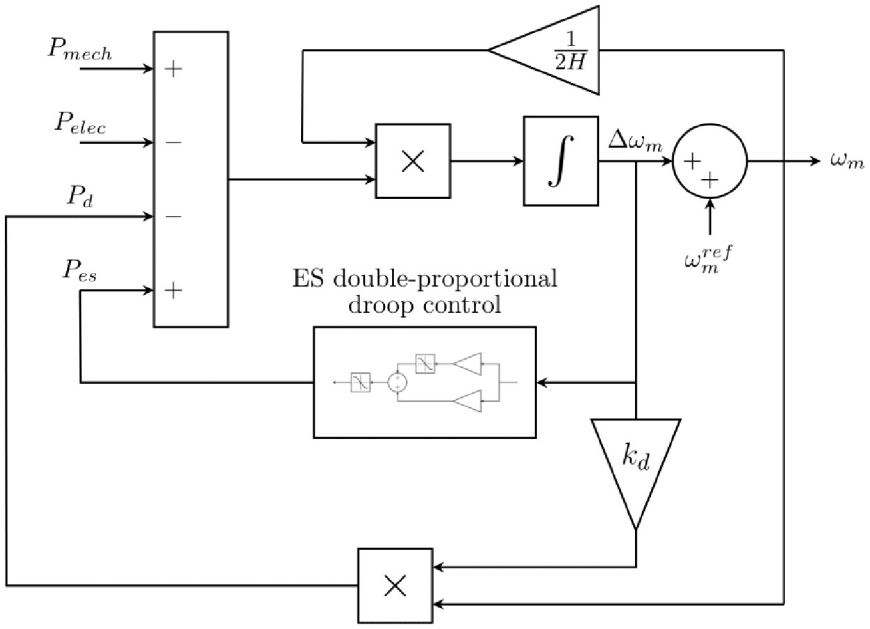

Fig. 7. Figure showing the control diagram of the Simulink model for evaluating the frequency control with ES.

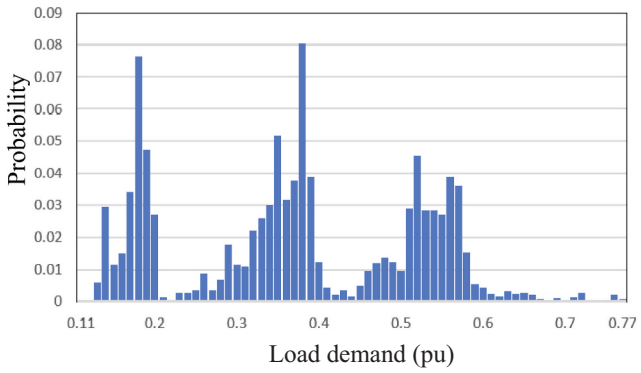

Fig. 8. Histogram of the selected platform load demand for a year.

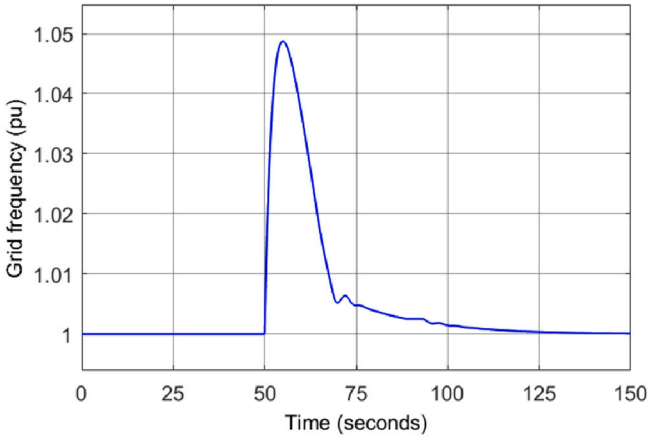

Fig. 9. Frequency control with a 0.0693 pu (7 MW) drop in load when load is at 0.2673 pu (27 MW).

motor was started when the load was <26.8 MW as a higher load will imply that 3 GTs have to be running to start the motor. Even if the load is higher than 26.8 MW, 3 GTs can be running to start the motor and one GT can be turned off after the motor start as long as the minimum up time of the GT is satisfied. Nevertheless, the focus is not on the motor start but on the turn off of the motor. A power rating that limits the frequency deviation to +0.05 pu was obtained to be roughly 3 MW. Fig. 9 shows the frequency control with a damping coefficient of 1.5 and power rating of 3 MW. The ES power during this transient event is shown in Fig. 10. The energy absorbed by the ES during the transient event of the 7 MW load drop was derived from the simulation to be 21.81 kWh. Thus, the usable energy is 21.81 kWh.

The minimum ES size is given in Eq. (12).

$$E_{min} = \frac{\eta_c \bullet E_{usable} + \frac{E_{usable}}{\eta_d}}{D_{deg}} \tag{12}$$

where E_{usable} is the total energy the ES must be able to absorb or release, η_c is the charging efficiency, η_d is the discharging efficiency, it is assumed that $\eta_c = \eta_d$ for all the four ES technologies, D_{deg} is the factor to account for capacity loss i.e. the ES must be able to deliver the rated energy at end of life, for SC $D_{deg} = 0.8$,for SMES, Li-ion and flywheel $D_{deg} = 1$. There is no capacity loss for flywheel and SMES and while Li-ion does undergo degradation the capacity loss is assumed to be negligible as the ES is significantly oversized. The values of η_c and η_d, the minimum ES size and other parameters used for the different ES technology are shown in Table 6. The overall efficiency in Table 6 includes not just the losses in the ES but also the losses in the power electronic converter. The efficiency of the ES and the efficiency of the power electronic converter in Table 6 is at a temperature of 25 °C and at least 50 % of rated power. The efficiency of the converter could be lower at lower power.

4.6. Space and weight of the ES technologies for the case study (step 5)

Now that the ES size has been determined, the practical space and weight implications of the sized ES are evaluated here. In the considered application, the ES weight limit is 50,000 kg and space limit is 120 m^2. Any ES technology that exceeds these hard limits will be discarded. Data for Helix power flywheel, Maxwell BCAP3400 P300 K04 SC [78] and SAFT Intensium Max+20 M Li-ion container battery [79] are used to compute the space and weight for the ES size in this case study. The dimension, weight and actual power/energy ratings for SC (Maxwell BCAP3400 P300 K04), Li-ion (SAFT Intensium Max+20 M) and flywheel (Helix power) are shown in Appendix C. For SMES it is hard to get practical data. However, SMES is known to require large space for large

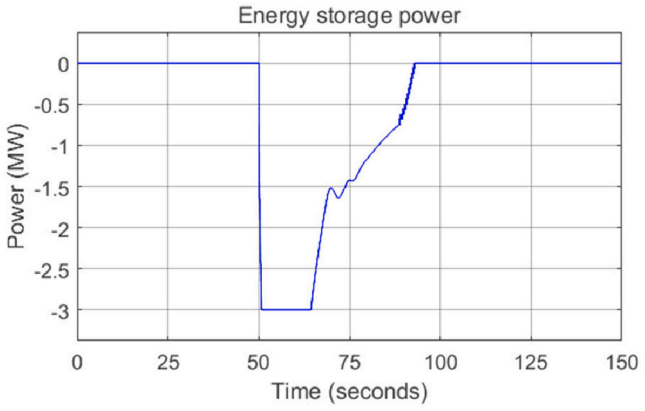

Fig. 10. Plot of the ES power during the 7 MW load drop.

energy ratings [80]. For example, a 160 km loop of coil is required for 1 GWh of energy [80]. Thus, the lowest gravimetric energy density (1 Wh/kg) and lowest volumetric energy density (0.2 kWh/m^3) given in Table 3 are used to estimate the weight and space for SMES. The power rating for the SAFT Li-ion battery is 2.5 MW. Since 3 MW is used in this case study and to create a fair comparison, the weight, space and volume of the actual battery container are scaled up by 20 % to account for the additional 0.5 MW.

For the power conditioning system, the weight and space are derived based on data of an SMA DC-DC converter [81] and SMA 4 MVA central inverter [82]. A 4 MVA inverter is used as it is the closest rating to the design rating (3.3 MVA). Note that the DC-DC converter is only used for supercapacitor. Five SMA DC-DC converters are used to achieve power rating of 3 MW. SMES and Li-ion use only the central inverter. The dimension for the power conditioning system is shown in Appendix C. The space for the flywheel power electronic converter is derived from the dimensions of the power electronic module in the Helix power flywheel datasheet. The weight of the HVAC is based on the typical weight of an air conditioner of 14 kW, 15 kW and 30 kW cooling power for SMES, SC, Li-ion respectively. The container weight for Li-ion is the empty weight of a 20-ft container. No container is used for SC, SMES and flywheel; it is assumed that an existing shelter on the platform can be used. The weight of the flywheel system is 20,412 kg (three Helix Power flywheels). Since the weight of the containment housing is up to half of the total flywheel weight [45,83,84] the weight of the containment housing can be expected to be around 10,206 kg. Table 7 shows the estimated weight for SC, SMES, Li-ion and flywheel. Table 8 presents the estimated volume, footprint and typical floor space for SC, SMES, Li-ion and flywheel. Floor space is the area required for the ES and this will usually be more than the ES footprint particularly for ES with many modules such as flywheel. Note that some of the figures in Tables 7 and 8 were calculated for an ES of 3 MW based on data obtained from the cited references. Fig. 11 shows the weight required for the sized ES while Fig. 12 shows the typical floor space required for the sized ES.

4.7. Life cycle cost analysis of high-power ES (step 6)

Here the life cycle cost of the ES technologies is evaluated. Since the four assessed ES technologies (flywheel, supercapacitor, SMES and Li-ion battery) in step 5 all meet the maximum weight and space constraints, they will all be considered in the life cycle cost analysis. The life cycle cost analysis evaluates all the associated costs of acquiring and operating a device over its design life, which includes initial capital cost, the present value of all replacements cost and the present value of operation and maintenance (O&M) cost throughout its design life. The capital cost is the cost of acquisition and installation, and it depends on the cost of the ES technology (cost per kW and cost per kWh). The replacement cost is the cost of all replacements over the project life and is adjusted with the interest rate to obtain the true cost.

Replacement is only done for SC since its life span is less than the project life, and it is done after its life span is exceeded. The O&M cost is the cost of all O&M services delivered over the design life of the ES and it is adjusted with inflation rate to get the true cost.

In estimating the total O&M cost, the cost of energy losses in the ES due to conversion losses (losses in ES and converter) and self-discharge/idling losses need to be computed. In particular, it is important to estimate the losses in the ES as they can be significant, e.g. 97 MWh was reported in losses in a 500-kW flywheel system on Flores Island, Portugal [85]. The OOGP load data was used to simulate the system shown in Fig. 7. The load data was trimmed down to only include load changes that cause 0.0025 pu change in the frequency (i.e. >1.48 MW for 4 GTs running, >1.11 MW for 3 GTs running and > 0.74 MW for 2 GTs running). This is done to reduce the simulation time. Another assumption made is that the load profile is similar from the first year to the last

Table 6
ES technology parameters (at 25 °C and 50 % of rated power).

ES Technology	SC	SMES	Li-ion	Flywheel
Self-discharge rate	40 %/day [21]	15 %/day [21]	0.1 %/day [21]	–
Efficiency of ES	96 % [21]	95 % [21]	95 % [21]	95 % [22]
Efficiency of Power converter	96 % * [81,82]	98 % [82]	98 % [82]	95 % *
Overall efficiency (the same for η_d and η_c)	92 %	93 %	93 %	90 %
Usable energy	21.81 kWh	21.81 kWh	21.81 kWh	21.81 kWh
Minimum Storage capacity	54.71 kWh	43.73 kWh	43.73 kWh	43.86 kWh
Minimum Power rating	3 MW	3 MW	3 MW	3 MW
Actual sized ES rating	3 MW/54.71 kWh [78]	3 MW/43.73 kWh	2.5 MW/1.1 MWh [79]	3 MW/75 kWh [22]
GT Damping factor	1.5			

* For SC and flywheel with two stage converter, converter efficiency is the overall efficiency of the two converters.

Table 7
Data for the ES practical weight for the case study.

ES technology	Supercapacitor	SMES	Li-ion (3 MW)	Flywheel
ES weight	8513 kg [78]	43,730 kg [21]	19,996 kg [79]	20,412 kg
Power conditioning system weight	6650 kg [81,82]	3700 kg [82]	3700 kg [82]	7400 kg [82]
HVAC/cooling system weight	269 kg	251 kg	537 kg	150 kg
Container weight	–	–	2300 kg	–
Containment housing	–	–	–	10,206 kg
Total ES system weight	15,432 kg	47,681 kg	26,533 kg	38,168 kg

Table 8
Data for the ES practical space for the case study.

ES technology	SC	SMES	Li-ion (3 MW)	Flywheel
ES volume	8.32 m^3 [78]	218.65 m^3 [21]	51.33 m^3 [79]	34.16 m^3*
Power conditioning system volume	18.94 m^3 [81,82]	10.23 m^3 [82]	10.23 m^3 [82]	19.84 m^3
HVAC/cooling system volume	6.82 m^3	6.37 m^3	13.65 m^3	2.92 m^3
ES footprint	3.33 m^2 ~ [78]	87.46 m^2 ~ [21]	17.72 m^2 [79]	14.01 m^2 +
Power conditioning system footprint	8.67 m^2	4.41 m^2 [82]	4.41 m^2 [82]	8.92 m^2
HVAC/cooling system footprint	2.73 m^2	2.55 m^2	- ^	2.67 m^2
Total ES system volume	34.08 m^3	235.25 m^3	75.21 m^3	56.92 m^3
Total ES system footprint	14.73 m^2	94.42 m^2	22.13 m^2	25.6 m^2
Typical ES system floor space	20 m^2	120 m^2	24.99 m^2	35 m^2

* ES volume for flywheel includes the containment housing.
+ ES footprint for flywheel includes the containment housing.
~ ES footprint for SC and SMES is computed assuming the height of the ES is 2.5 m.
^ No HVAC footprint for Li-ion as the HVAC is mounted on the container top.

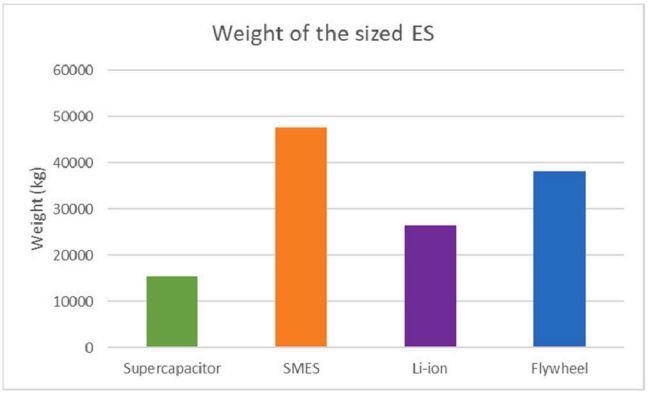

Fig. 11. Weight of the sized ES.

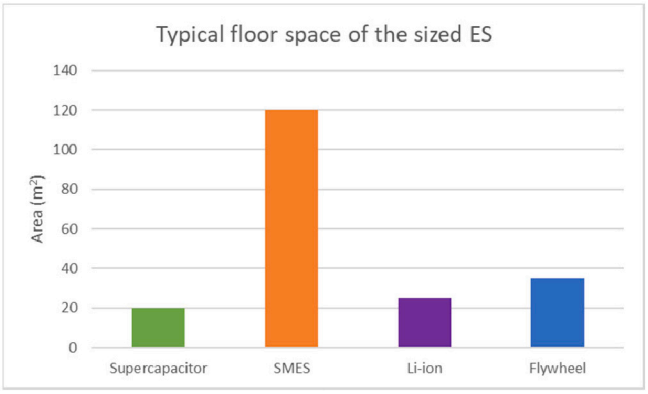

Fig. 12. Typical floor space required for the sized ES.

year of the project life. In practice, the load tends to decrease in OOGP from the early-life to mid-life and tail-life of the platform [20]. But this assumption is not expected to impact the analysis by much as the self-discharge/idling losses are significantly more than the non-ideal efficiency losses. From the simulation the total energy the ES exchanged with the grid is 2.055 MWh for a year. Table 9 shows the energy losses due to conversion losses, self-discharge losses and other losses for a year. Fig. 13 displays the total energy losses in the ES technologies over a period of one year.

The idling loss for SMES includes the power supplied to the cryogenic equipment to cool the superconductors. The idling loss for the flywheel includes the losses in the motor/generator, the self-discharge losses in the flywheel drive and the losses in the back-to-back power converter. In comparison, ABB's 500 kW flywheel was reported to have an average loss of 11 kW in [85], while [86] reported that the 1500 kW ABB flywheel has 15 kW idling losses. Note that for SC and Li-ion, the energy losses also include the power used to cool the SC and Li-ion. The power required for the HVAC for SC, SMES (cryogenic equipment) and Li-ion are shown in Table 9. In general, all the energy losses will be supplied by the GTs, thus the cost can be computed based on the fuel consumption data of the GE LM2500 and the price of natural gas.

The cost of the ES is determined by whichever is required between cost per kWh and cost per kW to achieve the desired rating. The ES rating cannot be achieved by using cost per kW for SC and SMES because SC and SMES can deliver very high power from very little storage capacity. Thus, cost per kWh is used, which achieves both the energy and power rating. For flywheel and Li-ion, the cost per kWh will achieve the energy rating but not the power rating, thus cost per kW is used, which achieves both energy and power rating. It must be noted that for all ES technol-

Table 9
Energy losses over one year.

ES technology	SC	SMES	Li-ion	Flywheel
Total energy absorbed	1.029 MWh			
Total energy released	1.026 MWh			
Total energy exchanged	2.055 MWh			
Non-ideal efficiency energy losses	0.17 MWh	0.15 MWh	0.15 MWh	0.22 MWh
Self-discharge energy losses	7.99 MWh	2.39 MWh	0.4 MWh	Included in idling losses
Converter standby losses	0.37 kW [82]	0.37 kW [82]	0.37 kW [82]	Included in idling losses
Total converter standby energy losses	3.24 MWh	3.24 MWh	3.24 MWh	Included in idling losses
Idling losses	–	–	–	29.7 kW[2]
Total idling energy losses	–		–	260.17 MWh
HVAC power	3.73 kW	4 kW[1]	8 kW	–
Total HVAC energy	32.7 MWh	35.04 MWh	70.08 MWh	–
Total energy losses	44.1 MWh	40.82 MWh	73.87 MWh	260.39 MWh

[1] The HVAC for SMES is the power consumed by the cryogenic equipment to cool the superconductors.
[2] 9.9 kW idling loss is assumed for each 1 MW flywheel unit based on what [47] reported.

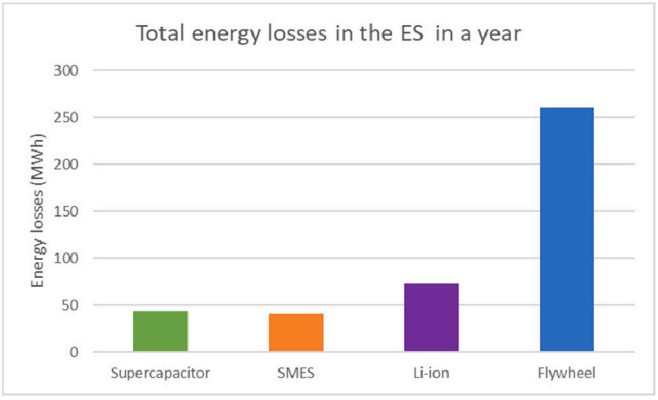

Fig. 13. Total energy losses in the ES technologies in a year.

ogies, it is hard to get a product in the market that will match the ES rating due to limited product modularity. Either the power rating will be oversized or the energy rating will be oversized. For SC and SMES, the power rating will be oversized while for flywheel and Li-ion, the energy rating will be oversized. Table 10 shows the cost parameters for the four ES technologies. Note that the project life for the considered case study is 20 years.

4.7.1. Life cycle cost

The life cycle cost (LCC) includes the initial capital cost, the total replacement cost and the total O&M cost. The LCC is given in Eq. (13).

$$LCC = C_{cap} + C_{rep} + C_{o\&m} \tag{13}$$

$$C_{rep} = RI_{cost} + C_{acrep} \bullet CRF \bullet Y_{proj} \bullet \sum_{j=1}^{N_{rep}} \frac{1}{(1+i)^{rep_{yrs}(j)\bullet j}} \tag{14}$$

$$CRF = \frac{i \bullet (i+1)^{Y_{proj}}}{(i+1)^{Y_{proj}} - 1} \tag{15}$$

$$C_{o\&m} = \sum_{l=1}^{Y_{proj}} C_{ann\_o\&m} \bullet (1+inf)^{Y_{proj}} \tag{16}$$

where *LCC* is life cycle cost, C_{cap} is the initial capital cost ($), C_{rep} is the present value cost of all replacements in the project life ($), RI_{cost} is replacement installation cost, $C_{o\&m}$ is the total O&M cost over the project life ($), C_{acrep} is the actual replacement cost, *CRF* is the capacity recovery factor, Y_{proj} is the project life in years, *N_rep* is the number of replacements, $rep\_yrs(j)$ is the number of years lasted before the j_{th} replacement (years), i is annual interest rate, $C_{ann\_o\&m}$ is the annual O&M cost and *inf* is annual inflation rate.

The total cost figures for the considered ES technologies are calculated using Eq. (13) to (16) and are shown in four pie charts in Fig. 14 a-d. The area of the pie chart is proportional to the LCC with SMES having the lowest LCC while Li-ion has the highest LCC. As can be seen from the pie charts, the replacement cost for SMES, Li-ion and flywheel is zero. The LCC is given in Table 11.

4.8. Decision-making on most suitable ES technology (step 7)

To make a decision on which ES is most suitable, a TSA table with the scores for the different attributes is created. The ES technology with the highest weighted TSA score is selected as the most suitable ES. Fig. 15 shows a chart with the relative relevance of the different attributes of ES for the selected test case, where grade 5 represents the highest relevance and grade 1 represents the lowest relevance. The ES attributes considered in the TSA table include weight, space, life cycle cost, safety and operational experience. The score for the weight and space is derived for the ES technologies based on the estimated weight and space in step 5 (section 4.5) of the TSA procedure. Likewise, the score for the LCC is derived from the result of the LCC analysis in step 6 (section 4.6) of the TSA procedure. The range of values used to determine the score for weight, space and life cycle cost are shown in Fig. 16, Fig. 17 and Fig. 18, respectively. The score for safety and operational experience are chosen subjectively. For safety, the score is chosen based on the state-of-the-art performance of the ES technologies with regards to safety. For operational experience, the score is chosen based on the review of operational experiences done in section 4.3. The overall weighted TSA score is given by Eq. (17). The weights used in Eq. (17) are obtained from Fig. 15.

Table 10
Cost parameters of the different ES technologies.

ES technology	Supercapacitor	SMES	Li-ion	Flywheel
Cost per usable kWh	$10,000 [28]	$10,000 [28]	–	–
Cost per kW	–	–	$686 [28]	$200 [28]
Cost of ES	$547,100	$437,300	$2,058,000	$600,000
Cost of Power converter	$279,750 [87]	$139,875 [87]	$139,875 [87]	$279,750 [87]
Cost of installation	$10,500 per tonne	$10,500 per tonne	$10,500 per tonne	$10,500 per tonne
Total cost of initial installation	$162,036	$500,651	$278,597	$405,395
Total cost of replacement installation	$89,387	–	–	–
Total capital cost	$988,886	$1,077,736	$2,476,472	$1,285,145
O&M cost for ES	0.5 % of cost of ES per year	2 % of cost of ES per year	0.5 % of cost of ES per year	2 % of cost of ES per year
O&M cost for Power converter	0.5 % of cost of power converter per year	0.5 % of cost of power converter per year	0.5 % of cost of power converter per year	0.5 % of cost of power converter per year
Energy loss per year	44.1 MWh	40.82 MWh	73.87 MWh	260.39 MWh
Cost of GT energy @30 % operational efficiency	$54.59/MWh based on Natural Gas price in June 2021 [88]			
Cost of energy loss	$2407/year	$2228/year	$4033/year	$14,215/year
O&M cost for ES and power converter	$3285/year	$8331/year	$10,989/year	$13,399/year
Total O&M cost	$5692/year	$10,559/year	$15,022/year	$27,614/year
Replacement cost of ES	$547,100	–	–	–
Life span of ES	12 years [21]	25 years [21]	20 years [79]	20 years [21]
Life span of Power converter	25 years [82]	25 years [82]	25 years [82]	25 years [82]
Project life	20 years			
Annual Interest rate	2 %			
Annual Inflation rate	1.2 %			

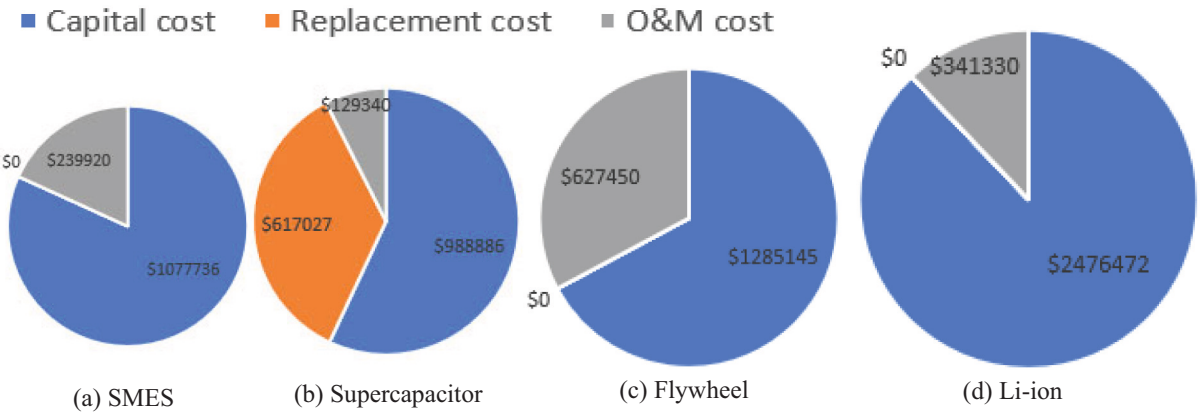

Fig. 14. Pie chart of the Life cycle cost of the four ES technologies.

Table 11
Life cycle cost of ES.

ES Technology	SMES	Supercapacitor	Flywheel	Li-ion
Life cycle cost	$1,317,656	$1,735,253	$1,912,595	$2,817,802

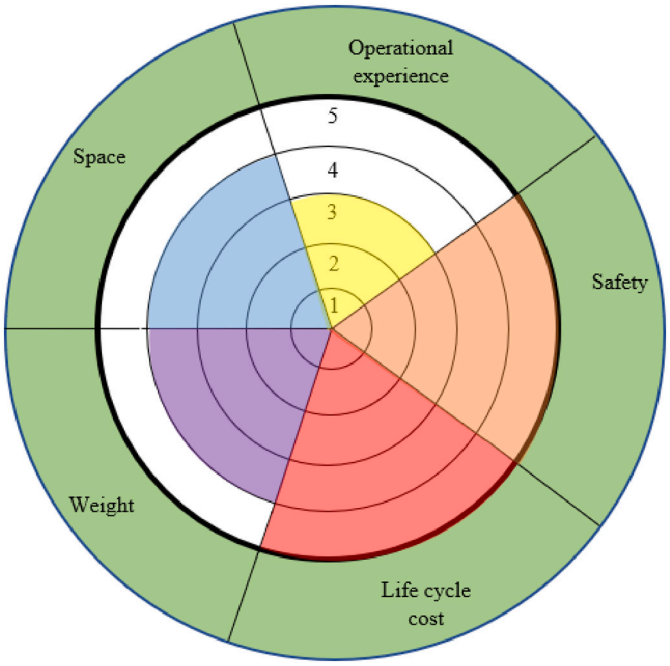

Fig. 15. The relative relevance of each criterium for TSA of the four ES technologies.

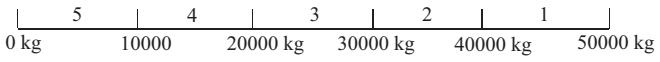

Fig. 16. Score range for weight.

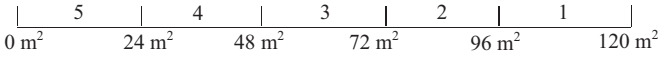

Fig. 17. Score range for space.

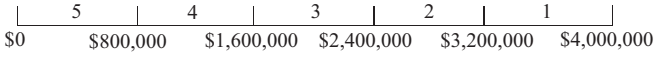

Fig. 18. Score range for life cycle cost.

Table 12 shows the score for the ES technologies for the five attributes and the overall TSA weighted score. From Table 12, it is evident that SCs have the highest weighted TSA score while SMES has the lowest weighted TSA score.

Fig. 19 shows a weighted chart based on the scores in Table 12 and the weights in Fig. 15. The score for ES weight and space in Fig. 19 can be any of the five values in [0.8, 1.6, 2.4, 3.2, 4]. The score for safety and LCC in Fig. 19 can be any of the five values in [1, 2, 3, 4, 5]. The score for operational experience in Fig. 19 can be any of the five values in [0.6, 1.2, 1.8, 2.4, 3]. For example, the score for SC for weight in Fig. 19 is 3.2. All these scores are according to applied weight.

This work has shown that there is a mismatch between ES technologies and the target application. For instance, it is apparent from the actual power and energy ratings of the ES technologies in Table 6 and Appendix C that no single ES is a perfect fit for the ES design. Either the power rating is oversized or the energy rating is oversized to ensure that both power and energy rating of ES design are achieved. This exemplifies why the TSA procedure is needed to select the most suitable ES.

In conclusion, SMES appears not to be suitable for this application as shown by its lowest weighted TSA score, due to its high weight and space. SMES is only good for services with small discharge time from milliseconds to 8 s [42] and is more suitable for uninterruptible power supply, voltage support, low-voltage ride through etc. Li-ion batteries have the second lowest weighted TSA score, and this is due to their poor performance in life cycle cost. Li-ion batteries can be a potential solution

$$TSA_{weighted} = \frac{4 \bullet weight + 4 \bullet space + 5 \bullet safety + 5 \bullet life\ cycle\ cost + 3 \bullet operational\ experience}{21} \quad (17)$$

Table 12
Technology suitability assessment weighted score.

Attributes	Supercapacitor	Flywheel	SMES	Li-ion
Weight	4	2	1	3
Space	5	4	1	4
Safety	5	5	5	4
Life cycle cost	3	3	4	2
Operational experience	3	4	3	5
Overall weighted TSA score	4.05	3.62	2.95	3.48

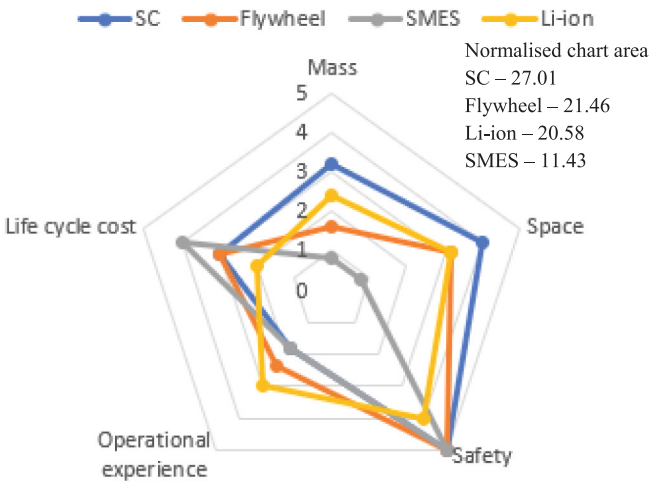

Fig. 19. TSA weighted chart of the four ES technologies.

where multiple services are considered. Li-ion battery can also be used in a hybrid ES solution where the Li-ion battery provides high energy and a high-power ES such as SC provides high power. Flywheels have the second-highest weighted TSA score and are a potential solution. Flywheels' high weighted TSA score is due to their good performance in operational experience, safety and space. SCs have the highest weighted TSA score with a good all-round performance and are therefore identified as the most suitable ES technology for primary frequency control, which requires high active power discharge in the considered OOGP.

5. Emerging energy storage technologies: Lithium-ion capacitor

To conclude the paper, a relatively new ES technology is introduced, which is the LiC recently developed by Beyonder in Norway [89]. Beyonder LiC has been chosen because they have one of the highest power density and energy density. This ES technology is assessed according to the same criteria as the previous ones, but results are kept in a separate section due to its significantly lower level of technological maturity.

LiC is a combination of a Li-ion cell and a capacitor to form a new ES technology that has the properties of a Li-ion battery and a SC. It combines the materials of Li-ion batteries and SC to form a new ES technology. It uses activated carbon made from saw dust in the cathode and lithium in the anode. One of the benefits of this technology is that it is very safe with reduced risk of thermal runaway in comparison with Li-ion chemistries. The use of activated carbon instead of metal oxide in the cathode completely eliminates the presence of oxygen internally that can support a potential fire. The LiC also has a very low internal resistance, which leads to less need for cooling and ultimately higher efficiency. It is rated to be able to deliver a C-rate of 30C, i.e., discharge/charge fully in just 2 min. This very high C-rate helps it achieve high power density, which will lead to it requiring small space and weight. The volumetric power density for the LiC is 18 kW/L and the gravimetric power density is 10 kW/kg. The volumetric energy density is 160 Wh/L, and the gravimetric energy density is 80 Wh/kg. It is also rated to be able to deliver 100,000 cycles.

Table 13
Lithium-ion capacitor weight.

ES size	ES weight	PCS[1] weight	HVAC weight	Total ES system weight
3 MW/102 kWh	4800 kg	6650 kg	269 kg	11,719 kg

[1] PCS – Power conditioning system.

Table 14
Lithium-ion capacitor space.

ES size	3 MW/102 kWh
ES volume	4.29 m^3
Power conditioning system volume	18.94 m^3
HVAC volume	6.82 m^3
ES footprint	1.99 m^2
Power conditioning system footprint	8.67 m^2
HVAC footprint	–
Total ES system volume	30.05 m^3
Total ES system footprint	10.66 m^2
ES system typical floor space	14 m^2

However, LiC are yet to see large scale application because the technology is not yet mature and also because it is expensive.

The weight and space for the LiC are estimated based on container dimension for 1 MW/34 kWh battery pack. Three containers are needed to achieve the total ES size required for the target application. The target application is the same as the one considered in the case study. The dimension and weight for the LiC container are given in Appendix C. The weight of the ES system is given in Table 13. The volume, footprint and typical floor space of the ES system are given in Table 14. It can be seen from Table 13 and Table 14 that the weight and space are even smaller than those obtained with the SC.

The lifespan of the LiC is 15 years. The ES size obtained through simulation in the case study (section 4.4) is used also here. Table 15 shows the ES size and cost parameters for LiC ES while Table 16 shows the LCC of the LiC. The energy loss of SC in Table 9 is used to determine the cost of energy loss of the LiC in Table 15. It can be seen from the LCC in Table 16 that the LiC is significantly cheaper than all the four ES technologies that have been reviewed. The small weight and space of the LiC and its very low LCC shows that it is the most promising ES for high-power applications if it can move from the product development cycle to commercial stage.

Table 16
Lithium-ion capacitor life cycle cost.

Capital cost	Replacement cost	O&M cost	Life cycle cost
$241,875	$215,748	$81,687	$539,310

Table 15
ES size and cost using lithium-ion capacitor.

ES size	Cost per kWh	ES Lifespan	ES cost	Converter cost	ES Replacement cost	O&M cost/year
3 MW/102 kWh	$1000/kWh	15 years	$102,000	$139,875 [84]	$102,000	0.5 % of Capital cost + $2386 (SC cost of energy loss is used from Table 10)

6. Conclusion

This paper proposed a TSA procedure. This procedure is general and can be used for assessing the suitability of ES technologies for various applications in the offshore environment. The most important criteria for applicability of ES in an OOGP environment include, among others, weight and space limitations, high safety, long life span and low maintenance requirements.

To exemplify the TSA procedure, a case study was considered where the targeted application is primary frequency control. SCs, flywheels, SMES and Li-ion were selected from a broader list of ES options.

The state of the art of these four ES technologies (SCs, flywheels, SMES and Li-ion) are provided in Appendix A. Operational experiences and practical deployments of these ES technologies for applications in the offshore and onshore environment were reviewed and their relevance was used to evaluate the feasibility of the four ES technologies assessed. The ES power and energy rating and the damping factor of the GTs were sized and, using these ES power and energy ratings, the weight and space required were estimated for SCs, flywheels, SMES and Li-ion. The ES sizing shows that there is no one-size-fits-all for any of the ES technologies and in all cases either the power or energy rating is oversized. The LCC analysis was then performed for the four ES technologies as they all meet the weight and space limit.

Furthermore, in the case study, a weighted TSA score was calculated for the four assessed ES technologies, where the attributes considered and weighted were ES weight, ES space, safety, LCC and operational experience. SMES had the lowest weighted TSA score despite having the lowest LCC, and this is due to its low score in weight and space. Li-ion had the second-lowest weighted TSA score due to its poor performance in LCC. Flywheels had the second-highest weighted TSA score, as they have good scores in operational experience, safety and space. From the LCC analysis, even though flywheels have reasonable capital investment and do not need replacement, they have very high O&M cost, due to their high operational energy losses, which will eventually make them an expensive solution. This is the only drawback of flywheels. In general, SCs have the highest weighted TSA score and are deemed as the most suitable ES solution for primary frequency control in the target application due to their high score in safety, weight and space. Note that the results of the case study depends on the inputs gathered about the ES technologies. However, the most important thing is the TSA methodology presented in this paper and the TSA analysis can always be re-run when more accurate inputs are obtained.

Finally, information on a new ES technology (LiC) was provided and practical weight and space, and LCC using this ES was estimated. The LiC has the smallest weight and space and also has the lowest LCC, thereby making it a very promising ES solution, which, if able to reach full commercialisation, could compete with SCs for services requiring high power applications with high C-rates.

CRediT authorship contribution statement

Ayotunde A. Adeyemo: Conceptualization, Methodology, Software, Writing - Original draft preparation, Writing - Reviewing and Editing. **Erick Alves:** Writing - Original draft preparation, Writing - Reviewing and Editing. **Francesco Marra:** Writing - Reviewing and Editing **Danilo Brandao:** Writing - Reviewing and Editing. **Elisabetta Tedeschi:** Methodology, Writing - Original draft preparation, Writing - Reviewing and Editing.

Declaration of competing interest

The authors declare no conflict of interest.

Data availability

The data that has been used is confidential.

Acknowledgments

This work was supported under the programme PETROMAKS2 of the Research Council of Norway within the project "Smart Platform" with grant number 308735.

Appendix A

A.1. Supercapacitor

SCs are special types of capacitors that use double-layer capacitance to store charge. They are also called electrostatic double-layer capacitors (ELDC). The double-layer is formed at the interface between a conducting carbon electrode and an electrolyte. Fig. A1 shows the diagram of a SC electrical structure.

The formula for an ideal capacitor is given by Eq. (A1).

$$C = \frac{\varepsilon_0 \bullet \varepsilon_r \bullet A}{d} \tag{A1}$$

where ε_0 is the permittivity of free space, ε_r is the relative permittivity of the dielectric, A is the effective surface area of the electrode, d is the separation of the two electrodes or the thickness of the dielectric and C is the capacitance of the capacitor.

Normal electrolytic capacitors usually have high power density but relatively low energy density in comparison to SCs. The ES capacity of a capacitor is directly proportional to its capacitance as given by Eq. (A2) below.

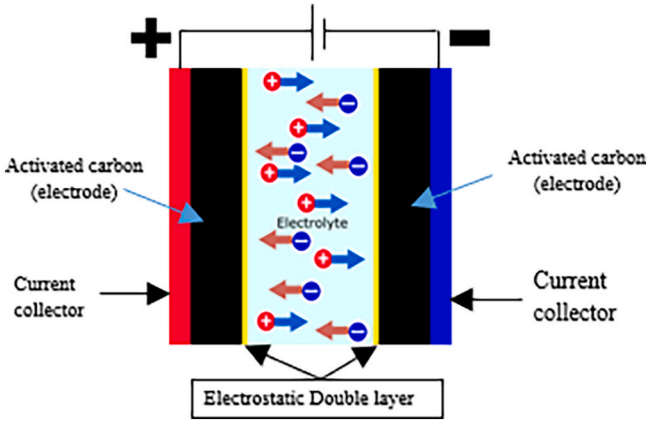

Fig. A1. Electrical structure of a supercapacitor (ELDC).

$$E_{sc} = 0.5 \bullet C \bullet V_{rated}^2 \tag{A2}$$

where V_{rated} is the rated voltage of the capacitor.

In order to increase the energy rating of a capacitor its capacitance has to be increased. Thus, SCs are designed with thick electrodes with very large surface area (such as activated carbon) and thin dielectrics which, combined together, yield capacitances and energy densities that can be up to thousands of times larger than those of electrolytic capacitors [90,91]. Two types of electrolytes are used for the ELDC: aqueous and organic electrolyte. The ELDC using aqueous electrolyte usually have a rated voltage of 0.9 V whereas the ELDC using organic electrolyte have rated voltage of 2.7 V. Thus, the organic electrolyte SCs have much higher energy density because of their higher rated voltage, but this comes at a cost of significantly higher price than the aqueous electrolyte SCs.

The simplest equivalent circuit model of a SC can be represented by a RC circuit where the capacitor models the ES capacity of the SC whereas the resistor models the power losses of the SC and is often referred to as the equivalent series resistance (ESR). However, a more elaborate equivalent circuit of a SC is that shown in Fig. A2. The ESR is the combination of the series resistance (Rs) and the parallel resistance (Rp). The parallel resistance only has impact for very low frequencies (millihertz range). The parallel resistance determines the leakage current of the SC (self-discharge rate) and should be of a high value so as to limit the leakage current.

The ESR and rated voltage of a SC determines the power and power density of a SC. For high power, it is desirable to have very low ESR. The peak power of a supercapacitor is given in Eq. (A3).

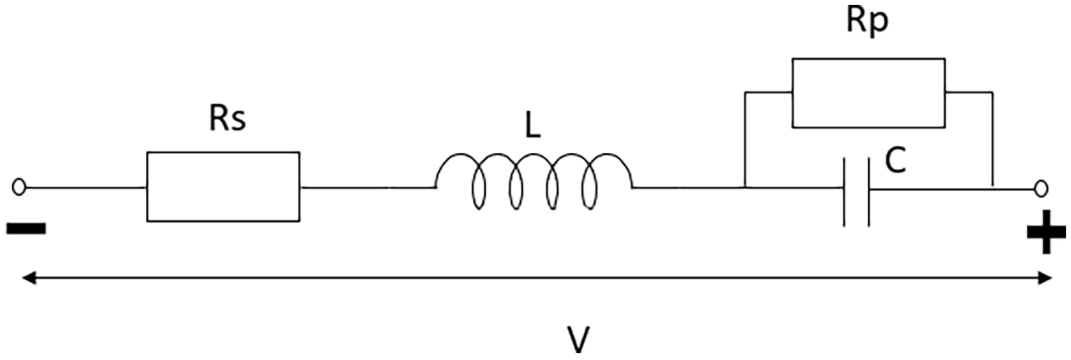

Fig. A2. Equivalent circuit of a supercapacitor.

$$P_{max} = \frac{V_{rated}^2}{4 \bullet ESR} \tag{A3}$$

where *ESR* is the equivalent series resistance.

However, the ESR of a SC is not a constant parameter as it varies with operating voltage, frequency and temperature. The ESR does not vary much with the operating voltage as it is largely similar for voltages between 2 and 2.7 V [92]. For lower voltages, the ESR gets slightly higher. The typical ESR of a SC is the average ESR over its operating voltage range. Eq. (A4) gives the usable energy of a SC.

$$E_{sc\_usable} = 0.5 \bullet C \bullet \left(V_{rated}^2 - (0.5 \bullet V_{rated})^2\right) \tag{A4}$$

From Eq. (A4) it can be seen that the operating voltage range of the SC is from full voltage to half the full voltage. The SC is not discharged below half its voltage to minimise the variation of the DC voltage feeding the power electronic converter. From Eq. (A4) the usable energy is 75 % of the total stored energy in the SC.

The variation of the ESR of a SC with frequency is shown in Fig. A3a [92]. It is evident that, for frequencies below 0.01 Hz, the ESR increases significantly. Thus, the DC ESR of a SC can be expected to be high. Increasing ESR values can also be seen for frequencies above 1000 Hz. The ESR of a

SC also increases significantly with temperature. The variation of the capacitance of a SC with frequency and voltage is shown in Fig. A3b and Fig. A3c, respectively. It can be seen that the capacitance for 0 Hz is close to rated value, but the capacitances drop significantly for frequencies above 0.1 Hz. In Fig. A3c it is evident that the capacitance of the SC increases with operating voltage.

The aging process of a SC increases with higher operating voltage and higher operating temperature. Since many SC cells are usually connected in series to achieve the rated voltage for the converter DC- link, it is clear that over-voltages need to be prevented using active balancing circuit. Additionally, operating a SC below its rated voltage can significantly increase its lifespan. However, reducing the operating voltage significantly reduces the usable energy since the ES of a SC varies with the square of the voltage. Thus, a trade-off must be found between energy density and lifespan.

Table A1 shows data for SC cells from different manufacturers. In general, the high energy density of SCs relative to conventional capacitors makes them suitable for ES solutions requiring fast response and large bursts of power, such as inertia frequency response services for grid, pulsed loads on ship and aircraft etc. The major advantages of SCs are high power density, long cycle life (>1000,000 cycles), high ramp rate and practically no maintenance requirement. They also do not need a special room like SMES, are portable and can work as plug and play. Additionally, SCs are inherently safe due to their low ESR thereby alleviating any thermal runaway concerns as in the case of Li-ion batteries. The major drawback of SCs is their relatively short lifespan in comparison with flywheels and SMES [21].

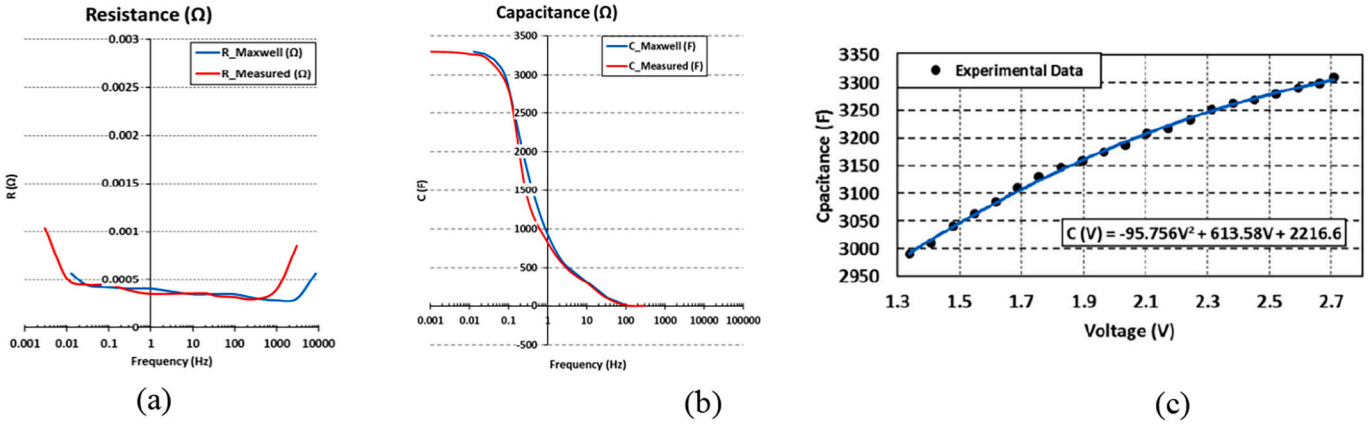

Fig. A3. (a) Plot of ESR of SC vs frequency (b) Variation of SC capacitance with frequency (c) Variation of SC capacitance with voltage. Adapted from [92].

Table A1
Supercapacitor cell data from different manufacturers.

Features	Maxwell [78]	Eaton [93]	Ioxus [94]	Yunasko [95]	Kamcap [96]
Rated voltage (V)	3.0	3.0	2.85	2.7	2.7
Initial rated capacitance (F)	3400	3000	3000	3000	3000
Initial ESR (mΩ)	0.15	0.23	0.2	0.14	0.29
Maximum current (A)	2800	2400	2700	2200	–
Usable specific power (kW/kg)	14.5	–	9.6	7.1	–
Peak specific power (kW/kg)	30	–	20	14.9	–
Peak specific power (kW/L)	–	–	25	–	–
Specific energy (Wh/kg)	8.57	7.38	6.6	6.2	–
Specific energy (Wh/L)	8.76	7.83	8.3	–	–
Operating temperature range (°C)	−40 to 65	−40 to 85	−40 to 65	−40 to 60	−40 to 65

A.2. Flywheels

Flywheels are also a good type of ES for fast power delivery. They store energy in the motion of a spinning disc. Fig. A4 shows the typical structure of a flywheel. The energy in a flywheel is expressed using Eq. (A5).

$$E_{fw} = \frac{1}{2} J_{fw} \bullet \omega_{fw}^2 \tag{A5}$$

where J_{fw} is the moment of inertia of the spinning disc, ω_{fw} is the angular speed of the disc.

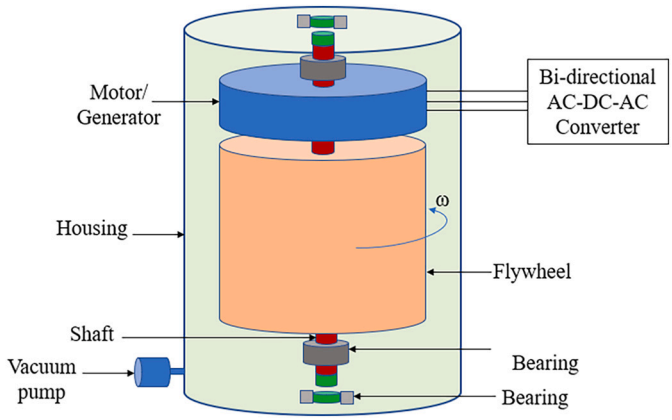

Fig. A4. Structure of a flywheel.

The flywheel ES is operated with a minimum angular velocity to limit the voltage variation and torque for a given power rating. The usable energy of the flywheel is given in Eq. (A6).

$$E_{fw\_usable} = \frac{1}{2} J_{fw} \bullet \left(\omega_{fw\_max}^2 - \omega_{fw\_min}^2 \right) \tag{A6}$$

where ω_{fw_max} is the maximum angular velocity and ω_{fw_min} is the minimum angular velocity.

The moment of inertia depends on the mass and geometry of the spinning mass. A solid cylindrical mass has a moment of inertia as given by Eq. (A7) while a hollow mass has a moment of inertia as given by Eq. (A8).

$$J_{fw} = \frac{1}{2} m \bullet r_c^2 \tag{A7}$$

$$J_{fw} = \frac{1}{2} m \bullet \left(r_o^2 - r_i^2 \right) \tag{A8}$$

where m is the mass of the spinning disc, r_c is the radius of the rotor material for a solid cylindrical mass, r_o is the outer radius of a hollow mass and r_i is the internal radius of a hollow mass.

The spinning disc is usually connected to a shaft supported with mechanical or magnetic bearings and spins in a vacuum to reduce windage losses. Mechanical bearings have friction losses and require more maintenance, while magnetic bearings have no friction losses and require little maintenance and are preferred for high-speed applications. From Eq. (A5) it is apparent that it is more beneficial to increase the ES capacity of a flywheel by increasing the speed of the disc than increasing the inertia/mass of the disc. However, the maximum speed a disc can support depends on the maximum stress that the rotor material can withstand (i.e., tensile strength), and this also depends on the shape of the rotor material [83,97]. Eq. (A9)–(A11) give the maximum stress, volumetric and gravimetric density of a flywheel.

$$\sigma_{max} = K \bullet \rho \bullet \omega_{fw}^2 \bullet r^2 \tag{A9}$$

$$E_v = K \bullet \sigma_{max} \left(J/m^3 \right) \tag{A10}$$

$$E_m = K \bullet \frac{\sigma_{max}}{\rho} \left(J/kg \right) \tag{A11}$$

where σ_{max} is the maximum stress, K is the shape factor, ρ is the density of the rotor material, r is the radius of the rotor material (for solid cylindrical mass $r = r_c$ and for hollow mass $r = r_o$), the linear speed is given by $\omega_{fw} \bullet r$, E_v is the energy per unit volume and E_m is energy per unit mass. The shape factors for some rotor shapes are given in Fig. A5 [83].

The flywheel must be operated with some margin of safety below the maximum stress. Note that these volumetric and mass energy densities are for the rotor material only and do not include other components of the flywheel. The overall energy densities can be expected to be much lower when the balance of plant is included.

Flywheels can be divided into two broad categories namely low-speed flywheels (ω_m<10,000 rpm) and high-speed flywheels (10,000 rpm < ω_m < 100,000 rpm). The low-speed flywheels are usually made with heavy metals while the high-speed flywheels are usually made with light composite materials that have high tensile strength. High-speed flywheels can be up to five times more expensive than low-speed flywheels [44,84]. Also, flywheels usually require a containment housing as a safety mechanism in case of failure of the flywheel. Many new flywheel designs (Stornetic [98] and Zooz [99]) are containerized in which a steel containment housing is built with the flywheel. In general, the containment housing of a flywheel increases the space and weight that the whole flywheel system takes and needs to be properly accounted for when technically assessing the viability of a flywheel system in an offshore environment. In fact, the weight of the containment housing can be up to half of the weight of the whole flywheel system for high-speed flywheels [45,83,84].

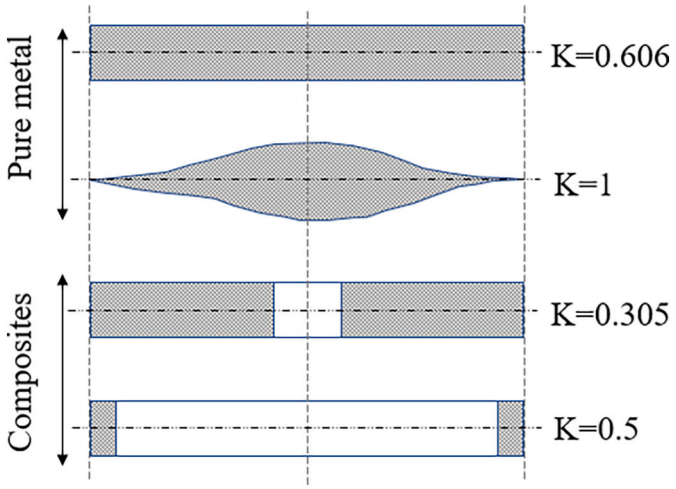

Fig. A5. Figure showing the shape factor of some rotor shapes.

A motor/generator machine is usually connected to the rotating shaft to charge or discharge the flywheel. The machine operates as a motor when storing energy from the grid thereby accelerating the flywheel while the machine releases energy to the grid when in the generator mode. Three types of machines are commonly used for such application: induction machines, synchronous machines and variable reluctance machines. In general, induction machines cannot operate at high speed and variable reluctance machines exhibit torque ripple, vibration and noise when used in high-speed flywheels. These torque ripples and vibration are undesirable for safe operation of the flywheel. Thus, permanent magnet synchronous machines are the most used for high-speed flywheels due to their flexible control, smooth torque, high power density and high efficiency (albeit this comes at a higher cost of the machine plus the associated cost of the power electronic converter) [83]. Additionally, the synchronous machine flywheel can be made to present real inertia that can deliver power instantaneously for frequency regulation services in grid applications, but this type of flywheel is usually very expensive [44]. A back-to-back AC-DC-AC power electronic converter configuration is typically used to interface the motor/generator machine. The grid side converter controls the DC-link voltage while the motor/generator side converter controls the operation of the flywheel. The cost of the power electronic converter for the flywheel is one of the major concerns for use of flywheels (as flywheels can be rated high up to several MW/MVA). However, the doubly fed induction machine (DFIM) has in recent times been making inroads into flywheel applications (albeit in low-speed flywheels) due to its requiring lower power electronic converter rating. This helps reduce the overall cost of the flywheel compared to using synchronous machines or other machine types. The DFIM flywheel are used more in high-power applications (several MVA) than the other machine types due to its lower cost.

Flywheels are modular in design and achieving a multi-MW configuration requires combining many flywheel units together. Each unit of a flywheel used for grid applications can be rated between 50 kW to 1.5 MW [22,85,86,98,100–102]. However, for special applications such as nuclear fusion, there are specially built high-power flywheels such as the two 400 MW flywheel at Culham Centre for Fusion Energy, UK [71]. The data for flywheel units for grid applications from some manufacturers are shown in Table A2. The rated power of the flywheel depends on the rating of the motor/generator and power conditioning system coupled to it.

The major advantages of flywheels are that they can be designed to meet different combinations of power and energy rating. Flywheels also have a long life span. Also, flywheels have high power density, high cycle life and very high ramp rate for power delivery. They have cheaper cost per energy capacity ($/kWh) than SCs and SMES (refer to Table 3). The most significant advantage of flywheels is that they do not require HVAC as a simple water-cooling system is usually sufficient for most designs. Like SCs, their energy density is low in comparison to battery and other ES technologies. The major drawback of flywheels is the high self-discharge rate. Also, the space required for flywheel's balance of plant could be significant.

A.3. Superconducting Magnetic Energy Storage

Superconducting magnetic ES is another potential high-power ES. It stores electric energy in a magnetic coil that is cryogenically cooled to temperatures as low as 1.8 K. The energy in the SMES can be expressed as in Eq. (A12).

$$E_{smes} = \frac{1}{2} \bullet L \bullet I^2 \tag{A12}$$

where L is the inductance of the coil and I is the current flowing into the superconducting coil.

Niobium-Titanium is often employed as a superconductor. The superconducting coil has negligible resistance at very low temperatures, which makes the efficiency of this ES very high, even higher than the efficiency of flywheels and SCs. Fig. A6 shows the typical structure of an SMES.

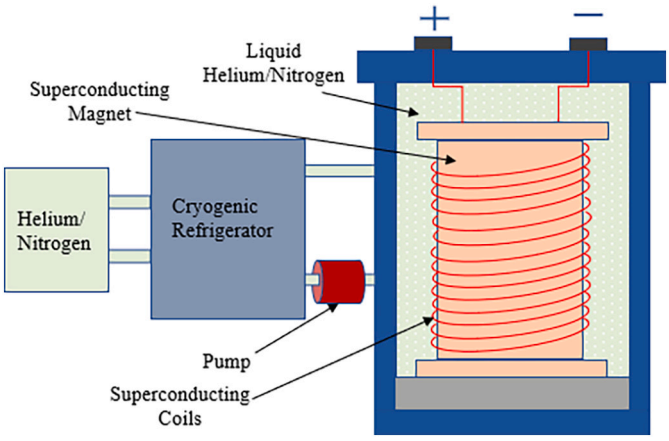

Fig. A6. Structure of an SMES.

The superconducting coil is usually interfaced with a DC-AC power converter that behaves as a rectifier when charging the SMES and as an inverter when discharging the SMES. The SMES is usually custom made and as a result practical data on it could not be provided. Although fast response is not considered in the case study in this work, it is worth mentioning that one of the main benefits of using SMES in grid applications is its fast response. It can respond for power delivery within 1 ms (depending on the power conditioning system interfaced with the SMES) and can go from charging to discharging in <10 ms. The SMES also has high power density and high cycle life. However, SMES is expensive and has significantly lower energy density compared to SCs and flywheels. Moreover, SMES requires a special room to house the cryogenic equipment and cannot be easily moved around upon installation. The most significant drawback with SMES is that it requires a lot of space as well as special care and handling. Also, pre-cooling of the conductor to superconducting temperature can take up to four months [103]. Thus, frequent maintenance and operational failures are highly discouraged as this will lead to a long downtime in operation of the ES. Also there has been a slow progress in SMES in the last two decades, and it is yet to become a proven technology of choice for high-power applications but SMES may become more relevant in future if progress is made in the development of low cost high temperature superconductors.

Table A2
Grid-scale/Micro-grid Flywheel Specifications from some manufacturers.

Manufacturer/ Model	Beacon Power – 400-300 [22]	ABB Powerstore [85,86]	Stornetic Durastor [98]	WattsUp Power's [100]	Adaptive power balancing [101]	Helix Power [102]
Rated Power	300 kW/360 kWp	500 kW, 1 MW and 1.5 MW	1 MW	100 kW	Configurable up to 5 MW with 16 flywheels	1 MW
Usable energy	30 kWh	5 kWh	64 kWh	–	12 kWh	25 kWh
Weight	5443 kg	–	28,000 kg	–	–	6804 kg
Angular speed	Up to 16,000 rpm	1800–3600 rpm	Up to 45,000 rpm	Up to 60,000 rpm	Up to 16,000 rpm	
Life cycle	175,000	–	>100,000	350,000	Unlimited	$>10^6$
Life span	25 years	–	–	–	25 years	20 years
Ramp rate	>1000 MW/min	–	–	–	–	
Response Time	1 ms	<5 ms at full reversal	–	–	<30 ms at full power reversal	
Recharge rate	Rated Power	Rated power	Rated power	–	–	
Efficiency	90–93 %	–	–	–	–	90–92 %
Self-discharge rate	2–3 % per hour	–	–	–	–	
Operating Temperature	-45 °C to 65 °C		–	–	–	-38 °C to 40 °C
Discharge Time	5 min for 300 kW)	–	260 s	–	–	90 s

A.4. Lithium-ion batteries

The only consolidated battery technology that can come close to the kind of performance that flywheels, SCs and SMES offer in short term high-power services is Li-ion batteries [21]. They have the highest power and energy density among the available battery technologies. The anode material is made of graphitic carbon. There are six main types of Li-ion batteries. Five of the six types vary depending on the cathode material used. The ones based on the cathode material are LFP, lithium nickel manganese cobalt, lithium nickel cobalt aluminium (NCA), $LiCoO_2$ and $LiMn_2O_4$. The sixth Li-ion battery, which has a different anode material to the other Li-ion battery chemistries, is LTO. Li-ion batteries store energy through the reversible movement of lithium ions through the electrolyte. When discharging, lithium ions move from the anode (releasing an electron) through the solid electrolyte interface to the cathode to form Li-salt at the cathode. The reverse takes place during charging, as lithium ions move from the cathode to the anode to combine with electrons.

One of the main concerns with some Li-ion battery chemistries is thermal runaway. Thus, extra protection circuit against over-voltage and thermal runaway is often required, which increases the cost of Li-ion batteries. NCA and $LiCoO_2$ have poor safety and cannot be used in an OOGP. In general, LFP and LTO are very safe. The LFP is even tolerant to physical abuse and is thus good for application in an OOGP.

A bi-directional power electronic converter is interfaced with Li-ion batteries to allow for charging and discharging of the battery. Li-ion battery chemistries differ in their performance characteristics, but they generally have lower power density and lower cycle life in comparison to flywheels, SCs and SMES [21,28]. However, Li-ion batteries have high energy density and high efficiency.

A.4.1. Lithium iron phosphate battery

LFP battery uses lithium iron phosphate in the cathode. One of the good features of LFP battery is its low resistance. Other advantages of LFP battery include high discharge C-rate (up to 25C) and long cycle life [104]. The major advantage of LFP battery compared to other Li-ion chemistries is its thermal stability with no risk of thermal runaway. Thus, LFP battery is a very safe choice for application in an OOGP. Furthermore, LFP battery are more tolerant to full charge voltage and shows significantly less degradation to full charge voltage compared to other Li-ion chemistries. However, LFP battery has higher self-discharge rate compared to other Li-ion chemistries and this can lead to balancing issues as the battery ages. This can be solved by using a robust cell balancing equipment but this increases cost. Also, LFP battery has lower specific energy compared to Li-ion chemistries that contains cobalt.

A.4.2. Lithium titanium oxide battery

LTO battery is the only Li-ion battery chemistry that does not use graphite in the anode, instead it uses LTO nanocrystals in the anode. Lithium manganese oxide or lithium nickel manganese cobalt oxide is used in the cathode. The use of nanocrystals in the anode increases the effective surface area and facilitate quick entry and exit of electrons in the anode. This facilitates high charge and discharge rate. Also, LTO battery is a better choice than graphite, due to its zero-strain property, no lithium plating while fast charging and charging under low temperature, thermal stability under high temperature and no solid electrolyte interface film formation. These properties lead to high cycle life for LTO battery. In addition, LTO battery is very safe and can operate in a wide temperature range. In particular, LTO battery has fantastic discharge characteristics under low temperature. However, LTO battery has low specific energy compared to other Li-ion chemistries due to its low nominal voltage (2.3 V). Also, LTO battery is the most expensive among Li-ion chemistries. LTO battery has found application in electric vehicle due to its ultra fast charging rate. However, it can also be used in an OOGP if cost is not an issue.

Appendix B

Table B1
Case study OOGP Grid Modeling parameter.

Parameter	Value	Parameter	Value
GT	GE LM2500	Proportional coefficient (Kp) for GTs secondary control	1.15
Apparent Power	25.25 MVA	Integral coefficient (Ki) for GTs secondary control	1.3
Active Power	20.2 MW	GTs primary control coefficient (Kp_droop)	16
Total OOGP capacity	101 MVA	Proportional coefficient (Kp1) for ES primary control	$^{200}/_{101}$
GE LM2500 Inertia constant	2.01 s	Proportional (Kp2) for ES primary control	$^{100}/_{101}$
Overall OOGP (4 GTs) Inertia constant	2.01 s	Proportional (Kp3) for avoiding frequency overshoot due to dynamic rate limiter	100
GE LM2500 maximum ramp rate	20 MW/min	Frequency deviation at which ES power reaches maximum	±0.02 pu
Total OOGP maximum ramp rate	Depends on how many GTs are online	GT Thermal power time constant	2.25
Damping factor	2.4	GT Governor Time constant	0.2

Appendix C

Table C1
Maxwell BCAP3400 P300 K04 supercapacitor [78].

Supercapacitor	Dimension	Energy	Weight	Volume	Actual footprint for a height of 2.5 m
Maxwell BCAP3400 P300 K04	6.1 cm dia × 16.6 cm	3.1875 Wh	0.496 kg	0.0004851 m^3	0.0029 m^2
Total for ES (17,164 units)		54.71 kWh	8513 kg	8.32 m^3	3.33 m^2

Table C2
SAFT Intensium Max+20 M Li-ion container battery [79].

Li-ion	Power/energy	Container dimension	Weight	Volume	Actual footprint
SAFT Intensium Max+20 M	2.5 MW/1.1 MWh	6.058 m × 2.438 m × 3.82 m	19,500 kg	56.42 m^3	14.77 m^2

Table C3
Flywheel weight and space for the sized ES based on Helix Power Flywheel.

Flywheel	Unit dimension	Weight	Volume	Actual footprint	Power/energy
Flywheel	6.75′ H × 5′ Dia	6804 kg	3.75* m^3	1.82* m^2	
Containment housing	8′ H × 8′ Dia	–	11.39 m^3	4.67 m^2	1 MW/25 kWh
Power electronics system	7.3′ H × 2′ W × 16′ D	–	6.61 m^3	2.97 m^2	
Heat exchanger	20.4″ H × 26.4″ W × 17″ D	–	0.15 m^3	0.29 m^2	
Coolant reservoir	54″ H × 31″ W × 30″	–	0.82 m^3	0.6 m^2	
Total for 1 unit		6804 kg	18.97 m^3	8.53 m^2	1 MW/25 kWh
Total for ES (3 units)		10,206 kg	56.91 m^3	25.59 m^2	3 MW/75 kWh

* Note that the volume and the footprint of the flywheel is included in the containment housing and is not added with the others to form the total.

Table C4
Lithium-ion capacitor weight and space.

Rating	1 MW/34 kWh Container
Dimension	865x738x2241mm
Weight	1600 kg

Table C5
SMA DPS-500 DC-DC converter parameters [81].

Power rating	600 kW at 1200 VDC to 1500 VDC
Dimension	850.9 × 2,044.7 × 1,000.8 mm
Weight	590 kg

Table C6
Sunny central 4000 UP-US Inverter parameters [82].

Power rating	4000 kVA at 35 °C
Dimension	2780 × 2,318 × 1,588 mm
Weight	3700 kg

References

[1] https://earth.org/what-countries-have-a-carbon-tax/ [Accessed on 27/03/2022].
[2] https://www.equinor.com/en/magazine/electrification-of-oil-and-gas-platforms.html [Accessed on 18/02/2022].
[3] https://www.offshore-energy.biz/benefits-and-challenges-of-offshore-platform-electrification/ [Accessed on 18/02/2022].
[4] E. Alves, S. Sanchez, D. Brandao, E. Tedeschi, Smart load management with energy storage for power quality enhancement in wind-powered oil and gas applications, Energies 12 (15) (2019) 2985.
[5] A.R. Årdal, K. Sharifabadi, Ø. Bergvoll, V. Berge, Challenges with integration and operation of offshore oil & gas platforms connected to an offshore wind power plant, in: 2014 Petroleum and Chemical Industry Conference Europe, IEEE, 2014, pp. 1–9.
[6] L.A. Vitoi, D. Brandao, E. Tedeschi, Active power filter pre-selection tool to enhance the power quality in oil and gas platforms, Energies 14 (4) (2021) 1024.
[7] I.C. Evans, M.J. Richards, The price of poor power quality, in: 2011 AADE National Technical Conference, 2011, pp. 1–17.
[8] I.C. Evans, The perils of offshore power quality. https://www.oedigital.com/news/444795-the-perils-of-offshore-power-quality, 2014 [Accessed 20/10/2022].
[9] IEC 61892-1, Mobile and Fixed Offshore Units – Electrical Installations – Part 1: General Requirements and Conditions, 2019.
[10] NORSOK, NORSOK Standard E-001, Electrical Systems, 6th ed., 2016.
[11] E.F. Alves, D.D. Mota, E. Tedeschi, Sizing of hybrid energy storage systems for inertial and primary frequency control, Front. Energy Res. 28 (9) (2021) 206.
[12] M.R. Aghamohammadi, H. Abdolahinia, A new approach for optimal sizing of battery energy storage system for primary frequency control of islanded microgrid, Int. J. Electr. Power Energy Syst. 1 (54) (2014) 325–333.
[13] V. Knap, S.K. Chaudhary, D.I. Stroe, M. Swierczynski, B.I. Craciun, R. Teodorescu, Sizing of an energy storage system for grid inertial response and primary frequency reserve, IEEE Trans. Power Syst. 31 (5) (2015) 3447–3456, https://doi.org/10.1109/TPWRS.2015.2503565.
[14] M. Sandelic, D.I. Stroe, F. Iov, Battery storage-based frequency containment reserves in large wind penetrated scenarios: a practical approach to sizing, Energies 11 (11) (2018) 3065.
[15] P. Moreno-Torres, M. Blanco, G. Navarro, M. Lafoz, Power smoothing system for wave energy converters by means of a supercapacitor-based energy storage system, in: 2015 17th European Conference on Power Electronics and Applications (EPE'15 ECCE-Europe), IEEE, 2015, pp. 1–9.
[16] Z. Zhou, F. Scuiller, J.F. Charpentier, M.E. Benbouzid, T. Tang, Power smoothing control in a grid-connected marine current turbine system for compensating swell effect, IEEE Trans. Sustain. Energy 4 (3) (2013) 816–826.
[17] D.B. Murray, J.G. Hayes, D.L. O'Sullivan, M.G. Egan, Supercapacitor testing for power smoothing in a variable speed offshore wave energy converter, IEEE J. Ocean. Eng. 37 (2) (2012) 301–308.
[18] S. Chapaloglou, D.I. Brandao, E. Tedeschi, Dynamic converter capacity allocation for multifunctional energy storage systems in oil and gas applications, in: 2021 Sixteenth International Conference on Ecological Vehicles and Renewable Energies (EVER), IEEE, 2021, pp. 1–10.
[19] S. Chapaloglou, D. Varagnolo, E. Tedeschi, Techno-economic evaluation of the sizing and operation of battery storage for isolated oil and gas platforms with high wind power penetration, in: IECON 2019-45th Annual Conference of the IEEE Industrial Electronics Society 1, IEEE, 2019, pp. 4587–4592.
[20] L. Riboldi, E.F. Alves, M. Pilarczyk, E. Tedeschi, L.O. Nord, Optimal design of a hybrid energy system for the supply of clean and stable energy to offshore installations, Front. Energy Res. 23 (8) (2020) 346.
[21] M. Farhadi, O. Mohammed, Energy storage technologies for high-power applications, IEEE Trans. Ind. Appl. 52 (3) (2015) 1953–1961.
[22] https://beaconpower.com/wp-content/uploads/2020/02/Beacon-Power-Model-400-300-Data-Sheet-Rev4.pdf. [Accessed 01/12/2021].
[23] https://www.ge.com/content/dam/gepower/global/en_US/documents/gas/gas-turbines/aero-products-specs/lm2500-50hz-fact-sheet-product-specifications.pdf [Accessed on 29/03/2021].
[24] J. Arseneaux, 20 MW Flywheel Frequency Regulation Plant, HazleSpindle LLC, Hazleton, PA, 2015 (United States), Tech. Rep.
[25] Beacon Power Inaugurates 20 MW Flywheel Plant in New York. https://www.power-grid.com/renewable-energy/beacon-power-inaugurates-20-mw-flywheel-plant-in-new-york/#gref, 2011 [Accessed 07/06/2022].
[26] N. Hamsic, A. Schmelter, A. Mohd, E. Ortjohann, E. Schultze, A. Tuckey, J. Zimmermann, Increasing renewable energy penetration in isolated grids using a flywheel energy storage system, in: 2007 International Conference on Power Engineering, Energy and Electrical Drives, IEEE, 2007, pp. 195–200.
[27] L. Zhou, Z. Qi, Modeling and simulation of flywheel energy storage system with IPMSM for voltage sags in distributed power network, in: 2009 International Conference on Mechatronics and Automation, IEEE, 2009, pp. 5046–5051.
[28] U. Akram, M. Nadarajah, R. Shah, F. Milano, A review on rapid responsive energy storage technologies for frequency regulation in modern power systems, Renew. Sust. Energ. Rev. 1 (120) (2020), 109626.
[29] J. Cerulli, G. Melotte, S. Peele, Operational experience with a superconducting magnetic energy storage device at Owens Corning Vinyl Operations, Fair Bluff, North Carolina, in: 1999 IEEE Power Engineering Society Summer Meeting. Conference Proceedings (Cat. No. 99CH36364) 1, IEEE, 1999, pp. 524–528.
[30] Nagata T, Hirano N, Nagaya S. SMES Development in Japan. http://b-dig.iie.org.mx/BibDig2/V13-0051/FORUM/FS4-3.pdf [Accessed on 20/08/2021].
[31] K. Prasertwong, N. Mithulananthan, D. Thakur, Understanding low-frequency oscillation in power systems, Int. J. Electr. Eng. Educ. 47 (3) (2010) 248–262.
[32] S. Sanchez, E. Tedeschi, J. Silva, M. Jafar, A. Marichalar, Smart load management of water injection systems in offshore oil and gas platforms integrating wind power, IET Renew. Power Gener. 11 (9) (2017) 1153–1162.
[33] C. Ma, S. Dong, J. Lian, X. Pang, Multi-objective sizing of hybrid energy storage system for large-scale photovoltaic power generation system, Sustainability 11 (19) (2019) 5441.
[34] F. Díaz-González, F.D. Bianchi, A. Sumper, O. Gomis-Bellmunt, Control of a flywheel energy storage system for power smoothing in wind power plants, IEEE Trans. Energy Convers. 29 (1) (2013) 204–214.
[35] G. Mandic, A. Nasiri, E. Ghotbi, E. Muljadi, Lithium-ion capacitor energy storage integrated with variable speed wind turbines for power smoothing, IEEE J. Emerging Sel. Top. Power Electron. 1 (4) (2013) 287–295.
[36] S.I. Gkavanoudis, C.S. Demoulias, A combined fault ride-through and power smoothing control method for full-converter wind turbines employing supercapacitor energy storage system, Electr. Power Syst. Res. 1 (106) (2014) 62–72.

[37] https://library.e.abb.com/public/5ead225120394decaaf7ede6407e922a/1KHA001315SEN1000_Microgrid%20reference%20list%20by%20year_08072015.pdf [Accessed on 30/11/2021].
[38] https://new.abb.com/news/detail/12807/abb-microgrid-solution-to-boost-renewable-energy-use-by-remote-community-in-kenya [Accessed on 30/11/2021].
[39] https://kenyaenergyfuture.wordpress.com/2015/09/14/kenya-first-flywheel-energy-storage-technology-to-be-set-up-in-marsabit/ [Accessed on 30/11/2021].
[40] https://www.hitachienergy.com/references/grid-edge-solutions/kodiak-island [Accessed on 30/11/2021].
[41] https://new.abb.com/docs/librariesprovider77/default-document-library/renewable-microgrids—reduced-lcoe-and-secure-power-supply—2016-08-25th—keabb-technology-day—light-version.pdf?sfvrsn=2 [Accessed on 30/11/2021].
[42] D.O. Akinyele, R.K. Rayudu, Review of energy storage technologies for sustainable power networks, Sustain. Energy Technol. Assess. 1 (8) (2014) 74–91.
[43] X. Luo, J. Wang, M. Dooner, J. Clarke, Overview of current development in electrical energy storage technologies and the application potential in power system operation, Appl. Energy 1 (137) (2015) 511–536.
[44] M.E. Amiryar, K.R. Pullen, A review of flywheel energy storage system technologies and their applications, Appl. Sci. 7 (3) (2017) 286.
[45] S. Choudhury, Flywheel energy storage systems: a critical review on technologies, applications, and future prospects, Int. Trans. Electr. Energy Syst. 31 (9) (2021), e13024.
[46] A.G. Olabi, T. Wilberforce, M.A. Abdelkareem, M. Ramadan, Critical review of flywheel energy storage system, Energies. 14 (8) (2021) 2159.
[47] X. Li, A. Palazzolo, A review of flywheel energy storage systems: state of the art and opportunities, J. Energy Storage 1 (46) (2022), 103576.
[48] B. Zakeri, S. Syri, Electrical energy storage systems: a comparative life cycle cost analysis, Renew. Sust. Energ. Rev. 1 (42) (2015) 569–596.
[49] Goris F, Severson EL. A review of flywheel energy storage systems for grid application. InIECON 2018-44th Annual Conference of the IEEE Industrial Electronics Society 2018 Oct 21 (pp. 1633-1639). IEEE.
[50] S. Brahim, S. Zhang, S. Maat, Fabrication and performance of supercapacitor devices using binder-free CNT electrodes, in: ECS Meeting Abstracts, IOP Publishing, 2018, p. 82. No. 1.
[51] V.G. Chirkin, N.A. Khripach, D.A. Petrichenko, B.A. Papkin, A review of battery-supercapacitor hybrid energy storage system schemes for power systems applications, Int. J. Mech. Eng. Technol. 8 (10) (2017) 699–707.
[52] K. Kovalev, V. Poltavets, I. Kolchanova, Flywheel energy storage systems for autonomous energy systems with renewable energy sources, in: IOP Conference Series: Materials Science and Engineering 643, IOP Publishing, 2019, p. 012106. No. 1.
[53] EPRI, Reassessment of superconducting magnetic energy storage (SMES) transmission system benefits, in: Electric Power Research Institute, Palo Alto, CA, USA, Tech. Rep, 2002.
[54] M. Khodaparastan, A. Mohamed, Flywheel vs. supercapacitor as wayside energy storage for electric rail transit systems, Inventions 4 (4) (2019) 62.
[55] G. Navarro, J. Torres, M. Blanco, J. Nájera, M. Santos-Herran, M. Lafoz, Present and future of supercapacitor technology applied to powertrains, renewable generation and grid connection applications, Energies 14 (11) (2021) 3060.
[56] D.B. Murray, M.G. Egan, J.G. Hayes, D.L. O'Sullivan, Applications of supercapacitor energy storage for a wave energy converter system, in: 8th European Wave and Tidal Energy Conference, 2009, pp. 786–795.
[57] Murray DB. Energy storage systems for wave energy converters and microgrids (Doctoral dissertation, University College Cork).
[58] J.N. Forestieri, M. Farasat, Integrative sizing/real-time energy management of a hybrid supercapacitor/undersea energy storage system for grid integration of wave energy conversion systems, IEEE J. Emerging Sel. Top. Power Electron. 8 (4) (2019) 3798–3810.
[59] Zhou Z. Modeling and power control of a marine current turbine system with energy storage devices (Doctoral dissertation, Université de Bretagne occidentale-Brest).
[60] W. Chen, A.K. Ådnanses, J.F. Hansen, J.O. Lindtjørn, T. Tang, Super-capacitors based hybrid converter in marine electric propulsion system, in: The XIX International Conference on Electrical Machines-ICEM 2010, IEEE, 2010, pp. 1–6.
[61] R. Kopka, W. Tarczyński, A fractional model of supercapacitors for use in energy storage systems of next-generation shipboard electrical networks, J. Mar. Eng. Technol. 16 (4) (2017) 200–208.
[62] J. Hou, J. Sun, H. Hofmann, Mitigating power fluctuations in electrical ship propulsion using model predictive control with hybrid energy storage system, in: 2014 American Control Conference, IEEE, 2014, pp. 4366–4371.
[63] J. Hou, J. Sun, H.F. Hofmann, Mitigating power fluctuations in electric ship propulsion with hybrid energy storage system: design and analysis, IEEE J. Ocean. Eng. 43 (1) (2017) 93–107.
[64] W.V. Hassenzahl, D.W. Hazelton, B.K. Johnson, P. Komarek, M. Noe, C.T. Reis, Electric power applications of superconductivity, Proceedings of the IEEE 92 (10) (2004) 1655–1674 [Accessed 07/06/2022].
[65] https://www.neces.com/project/laurel-mountain-wv-32-mw-8-mwh/ [Accessed on 28/03/2022].
[66] J. Kim, Y. Suharto, T.U. Daim, Evaluation of electrical energy storage (EES) technologies for renewable energy: a case from the US Pacific northwest, J. Energy Storage 1 (11) (2017) 25–54.
[67] S. Molina, E. Nicolas, M. Trabelsi, F. Sculiller, J.F. Charpentier, C. Franquet, A real scale prototype to smooth short-time power fluctuations of marine renewable energy sources-Uliss. EMR Project, in: 2019 Offshore Energy and Storage Summit (OSES), IEEE, 2019, pp. 1–6.
[68] S. Nagaya, N. Hirano, M. Kondo, T. Tanaka, H. Nakabayashi, K. Shikimachi, S. Hanai, J. Inagaki, S. Ioka, S. Kawashima, Development and performance results of 5 MVA SMES for bridging instantaneous voltage dips, IEEE Trans. Appl. Supercond. 14 (2) (2004) 699–704.
[69] A.T. Kearney Energy Transition Institute. Electricity Storage Gaining Momentum. https://www.energy-transition-institute.com/documents/17779499/17781903/Electricity Storage_FactBook.pdf/671389f7-6206-3bd9-50dd-4d214cf77871?t=1561052363812 [Accessed on 18/08/2021].
[70] I. Mexis, G. Todeschini, Battery energy storage systems in the United Kingdom: a review of current state-of-the-art and future applications, Energies. 13 (14) (2020) 3616.
[71] D. Rendell, S.R. Shaw, P.J. Pool, C. Oberlin-Harris, JET EFDA Contributors, Thirty Year Operational Experience of the JET Flywheel Generators, EFDA JET, 2014.
[72] J. Schmeller, R. Hockney, M. Polimeno, J. McGroarty, Flywheel energy storage system for electric start and an all-electric ship, in: IEEE Electric Ship Technologies Symposium, 2005, IEEE, 2005, pp. 400–406.
[73] M.I. Daoud, A. Massoud, S. Ahmed, A.S. Abdel-Khalik, A. Elserougi, Ride-through capability enhancement of VSC-HVDC based wind farms using low speed flywheel energy storage system, in: 2014 IEEE Applied Power Electronics Conference and Exposition-APEC 2014, IEEE, 2014, pp. 2706–2712.
[74] H.W. Jeong, Y.S. Ha, Y.S. Kim, C.H. Kim, K.K. Yoon, D.H. Seo, Shore power to ships and offshore plants with flywheel energy storage system, J. Adv. Mar. Eng. Technol. 37 (7) (2013) 771–777.
[75] T. Nakken, E. Frantzen, E.F. Hagen, H. Strom, Utsira—demonstrating the renewable hydrogen society, in: World Hydrogen Energy Conference 16, 2006.
[76] Verve Energy, Coral Bay Wind Diesel System—Information Sheet, Perth, Western Australia, 2008.
[77] J. Machowski, J.W. Bialek, J.R. Bumby, Power System Dynamics: Stability and Control, 2nd ed., Wiley, Chichester, UK, 2008. OCLC: Ocn232130756.
[78] https://maxwell.com/wp-content/uploads/2021/08/3V_3400F_datasheet.pdf [Accessed on 25/10/2022].
[79] http://www.efo-power.ru/datasheet/Saft/System/IM_20M.pdf [Accessed on 01/12/2021].
[80] https://www.chemeurope.com/en/encyclopedia/Superconducting_magnetic_energy_storage.html.
[81] https://files.sma.de/downloads/DC-DC-CONVERT-DS-en-12.pdf [Accessed on 06/05/2022].
[82] https://files.sma.de/downloads/SCXXXX-UP-US-DS-en-23.pdf?_ga=2.43631909.1021998441.1651681208-1360543306.1651681208 [Accessed on 06/05/2022].
[83] R. Pena-Alzola, R. Sebastián, J. Quesada, A. Colmenar, Review of flywheel based energy storage systems, in: 2011 International Conference on Power Engineering, Energy and Electrical Drives, IEEE, 2011, pp. 1–6.
[84] S. Karrari, M. Noe, J. Geisbuesch, High-speed flywheel energy storage system (FESS) for voltage and frequency support in low voltage distribution networks, in: 2018 IEEE 3rd International Conference on Intelligent Energy and Power Systems (IEPS), IEEE, 2018, pp. 176–182.
[85] André P. Integration of Flywheels in the Electrical System with the Aim of Maximising the Penetration Of Renewable Energy. XIICLEEE – 12th Portuguese-Spanish Conference on Electrical Engineering. http://b-dig.iie.org.mx/BibDig2/P11-0348/Communications/XIICLEEE_2037.pdf [Accessed on 17/11/2021].
[86] http://www.energystorage-cdt.ac.uk/outputs/cohort-1/Thomas Bryden - mini project.pdf [Accessed on 01/12/2021].
[87] K. Padmanathan, U. Govindarajan, V.K. Ramachandaramurthy, T. Sudar Oli Selvi, Multiple criteria decision making (MCDM) based economic analysis of solar PV system with respect to performance investigation for Indian market, Sustainability 9 (2017) 820.
[88] https://www.eia.gov/dnav/ng/hist/n3035us3m.htm [Accessed on 18/02/2022].
[89] https://www.beyonder.no/technology [Accessed on 28/02/2022].
[90] B. Roberts, Capturing grid power, IEEE Power Energ. Mag. 7 (4) (2009) 32–41.
[91] P. Sharma, T.S. Bhatti, A review on electrochemical double-layer capacitors, Energy Convers. Manag. 51 (12) (2010) 2901–2912.
[92] G. Navarro, J. Nájera, J. Torres, M. Blanco, M. Santos, M. Lafoz, Development and experimental validation of a supercapacitor frequency domain model for industrial energy applications considering dynamic behaviour at high frequencies, Energies. 13 (5) (2020) 1156.
[93] Eaton XL60 Technical data sheet. https://www.eaton.com/content/dam/eaton/products/electronic-components/resources/data-sheet/eaton-xl60-supercapacitors-cylindrical-cells-data-sheet.pdf. [Accessed 20/08/2021].
[94] Ioxus iRD3000F285CT Datasheet. https://ioxus.com/wp-content/uploads/2021/01/DataSheet_60mm_Cells_200316.pdf. [Accessed on 20/08/2021].
[95] Yunasko. https://yunasko.com/images/data/YUNASKO_Datasheet_cell_3000F_E.pdf. [Accessed on 20/08/2021].

[96] KAMCAP Power, KAMCAP Supercapacitors, Available online: https://www.kamcappower.com/products/winding-type-2.7-volt-super-capacitors/ [Accessed on 27 January 2021].
[97] R. Östergård, Flywheel Energy Storage: A Conceptual Study, Uppsala Universitet, Uppsala, Sweden, 2011. Master's Thesis.
[98] https://stornetic.com/assets/downloads/stornetic_general_presentation.pdf [Accessed on 01/12/2021].
[99] https://www.zoozpower.com/ [Accessed 16/11/2022].
[100] https://wattsuppower.com/flywheel/ [Accessed on 01/12/2021].
[101] https://www.adaptive-balancing.de/en/product/ [Accessed on 01/12/2021].
[102] https://www.helixpower.com/ [Accessed 21/10/2022].
[103] M. Noe, M. Steurer, High-temperature superconductor fault current limiters: concepts, applications, and development status, Supercond. Sci. Technol. 20 (3) (2007) R15.
[104] https://batteryuniversity.com/article/bu-205-types-of-lithium-ion. [Accessed 25/03/2022].